UC Irvine
UC Irvine Previously Published Works

Title

Biogenic emission measurement and inventories determination of biogenic emissions in the eastern United States and Texas and comparison with biogenic emission inventories

Authors

Warneke, C
de Gouw, JA
Del Negro, L
et al.

Biogenic emission measurement and inventories determination of biogenic emissions in the eastern United States and Texas and comparison with biogenic emission inventories

C. Warneke,[1,2] J. A. de Gouw,[1,2] L. Del Negro,[3] J. Brioude,[1,2] S. McKeen,[1,2] H. Stark,[1,2] W. C. Kuster,[1] P. D. Goldan,[1] M. Trainer,[1] F. C. Fehsenfeld,[1,2] C. Wiedinmyer,[4] A. B. Guenther,[4] A. Hansel,[5] A. Wisthaler,[5] E. Atlas,[6] J. S. Holloway,[1,2] T. B. Ryerson,[1] J. Peischl,[1,2] L. G. Huey,[7] and A. T. Case Hanks[8]

[1] During the NOAA Southern Oxidant Study 1999 (SOS1999), Texas Air Quality Study 2000 (TexAQS2000), International Consortium for Atmospheric Research on Transport and Transformation (ICARTT2004), and Texas Air Quality Study 2006 (TexAQS2006) campaigns, airborne measurements of isoprene and monoterpenes were made in the eastern United States and in Texas, and the results are used to evaluate the biogenic emission inventories BEIS3.12, BEIS3.13, MEGAN2, and WM2001. Two methods are used for the evaluation. First, the emissions are directly estimated from the ambient isoprene and monoterpene measurements assuming a well-mixed boundary layer and are compared with the emissions from the inventories extracted along the flight tracks. Second, BEIS3.12 is incorporated into the detailed transport model FLEXPART, which allows the isoprene and monoterpene mixing ratios to be calculated and compared to the measurements. The overall agreement for all inventories is within a factor of 2 and the two methods give consistent results. MEGAN2 is in most cases higher, and BEIS3.12 and BEIS3.13 lower than the emissions determined from the measurements. Regions with clear discrepancies are identified. For example, an isoprene hot spot to the northwest of Houston, Texas, was expected from BEIS3 but not observed in the measurements. Interannual differences in emissions of about a factor of 2 were observed in Texas between 2000 and 2006.

1. Introduction

[2] A large number of different volatile organic compounds (VOCs) are emitted into the atmosphere by the biosphere with a total of about 1150 Tg C yr^{-1} [*Guenther et al.*, 1995], which represents about 80% of the total global VOC emissions. These emissions are dominated by isoprene with an estimated global annual emission of 440–660 Tg C yr^{-1} [*Guenther et al.*, 2006]. Other large biogenic emissions include various monoterpenes with a combined emission of about 127 Tg C yr^{-1} [*Guenther et al.*, 1995], methanol with about 100–160 Tg yr^{-1} [*Jacob et al.*, 2005], and acetone with about 33 Tg yr^{-1} [*Jacob et al.*, 2002]. While the emissions of isoprene and monoterpenes have been extensively studied, large uncertainties remain for many regions and most other species.

[3] Because of the enormous impact of biogenic VOC emissions on the global and regional atmospheric chemistry producing ozone and secondary organic aerosol [*Henze and Seinfeld*, 2006; *Pfister et al.*, 2008], biogenic VOCs are included in air quality forecast models, global chemistry and climate models and in regulatory regional models. The model input is usually in the form of off-line emission inventories. The most commonly used biogenic emissions model in United States is the EPA BEIS3 (Environmental Protection Agency Biogenic Emissions Inventory System 3) (http://www.epa.gov/asmdnerl/biogen.html), which includes

---

[1]Chemical Sciences Division, ESRL, NOAA, Boulder, Colorado, USA.
[2]CIRES, University of Colorado at Boulder, Boulder, Colorado, USA.
[3]Department of Chemistry, Lake Forest College, Lake Forest, Illinois, USA.
[4]ACD, NCAR, Boulder, Colorado, USA.
[5]Institut für Ionenphysik und Angewandte Physik, Universität Innsbruck, Innsbruck, Austria.
[6]Marine and Atmospheric Chemistry Division, Rosenstiel School of Marine and Atmospheric Sciences, University of Miami, Miami, Florida, USA.
[7]School of Earth and Atmospheric Sciences, Georgia Institute of Technology, Atlanta, Georgia, USA.
[8]Department of Geosciences, University of Louisiana at Monroe, Monroe, Louisiana, USA.

isoprene, the monoterpenes and many other species. Another model, recently introduced by *Guenther et al.* [2006], is called MEGAN2 (Model of Emissions of Gases and Aerosols from Nature version 2), which is a detailed global model for isoprene and more than 100 other VOCs. MEGAN2 is publicly available at http://cdp.ucar.edu.

[4] Biogenic emission inventories have been evaluated in a number of different ways. Above-canopy flux measurements using eddy covariance techniques have been used frequently [*Guenther and Hills*, 1998]. Such studies allow a very detailed evaluation of the parameterization of biogenic emissions versus light, temperature and other parameters used in the inventories, but do this for one location only. Second, inverse modeling or indirect methods have been used to test biogenic emission inventories. For example, *Millet et al.* [2008] used formaldehyde columns derived from the Ozone Monitoring Instrument (OMI) to derive isoprene emissions over North America, which were 4–25% lower than predicted by MEGAN2. Earlier, formaldehyde retrievals from GOME were used to estimate isoprene emissions with similar results [*Palmer et al.*, 2006]. With the same method, but SCIAMACHY formaldehyde data, *Stavrakou et al.* [2009] estimate isoprene emissions about 40% lower than MEGAN2 for North America. *Muller et al.* [2008] used MEGAN2 in a global model using ECMWF meteorology and a detailed canopy environment model and found an underprediction of the modeled isoprene flux by about 30% for the Harvard forest site. Isoprene has recently been modeled in Texas for two flights from the TexAQS2000 campaign using the Comprehensive Air Quality Model with Extensions and the Global Biosphere Emissions and Interactions System (GLOBEIS) [*Song et al.*, 2008]. An overprediction was found for areas with high isoprene mixing ratios and underpredictions for areas with low isoprene mixing ratios. Many different variables, such as boundary layer height, temperature, photosynthetically active radiation (PAR), and chemistry, have to be modeled correctly for a model-measurement comparison to be successful, which makes these direct comparisons very challenging. Only recently have results been published that use aircraft measurements on a somewhat larger spatial scale to quantitatively derive isoprene emissions and compare to emission inventories. For example, *Karl et al.* [2007] found measured isoprene fluxes derived from aircraft measurements about 40% higher than predicted by MEGAN2 over Amazonia.

[5] During the NOAA SOS1999, TexAQS2000, ICARTT2004 and TexAQS2006 campaigns, multiple flights were performed covering many forested areas in the eastern United States and Texas. In this work we use the in situ measurements of isoprene and monoterpenes from those field campaigns in an attempt to evaluate the available biogenic emission models EPA BEIS3.12, the latest version EPA BEIS3.13, MEGAN2 and a model developed by *Wiedinmyer et al.* [2001] for Texas only (WM2001). Two approaches are used for this evaluation. First, the emissions are estimated from the ambient measurements assuming a well-mixed boundary layer, an entrainment flux and chemical loss due to OH, and compared to the emissions from the inventories extracted along the flight tracks in the boundary layer. Second, BEIS3.12 was incorporated into the Lagrangian transport model FLEXPART, and the calculated iso-

prene and monoterpene mixing ratios are compared to the aircraft measurements.

## 2. Airborne Measurements of Biogenic VOCs in the United States

2.1. Measurement Campaigns: SOS1999, TexAQS2000, ICARTT2004, and TexAQS2006

[6] Airborne measurements of biogenic VOCs were conducted in the framework of four different summertime campaigns: the Southern Oxidants Study 1999 (SOS99) in June and July of 1999 in the southeast United States [*Brock et al.*, 2002], the Texas Air Quality Study in August and September 2000 (TexAQS2000) [*Ryerson et al.*, 2003] and the Texas Air Quality Study in September and October of 2006 (TexAQS2006) [*Parrish et al.*, 2009] also in Texas, and the ICARTT2004 study in July and August of 2004 in the northeast United States [*Fehsenfeld et al.*, 2006]. Isoprene was measured during all four campaigns, the sum of the monoterpenes during ICARTT2004 and TexAQS2006. For the work presented here, we will use only the data obtained in the boundary layer.

[7] The flight tracks of the NOAA WP-3 for SOS99, ICARTT2004 and TexAQS2006 campaigns are shown in Figure 1a on top of the EPA BEIS3.13 summer isoprene base emissions map of the United States. Base emissions are the isoprene emissions at standard conditions (30°C and 1000 μmol m^{-2} h^{-1} for all leaves). Actual emissions deviate from the base emissions as a function of temperature and light, as will be discussed in detail below. Flight tracks in the boundary layer are shown in black, the ones in the free troposphere in red. It can be seen that the area covered by the flight tracks includes a large part of the forested eastern half of the United States including Texas, where large isoprene emissions are predicted. The flight tracks of the TexAQS2000 study are shown in Figure 1b on top of the MEGAN2 isoprene base emission factors. In Figure 1c the BEIS3.13 summer monoterpene base emissions are shown.

2.2. Instrumentation

[8] During the ICARTT2004 and TexAQS2006 campaigns, isoprene, and its oxidation products methyl vinyl ketone (MVK) and methacrolein (MACR), and monoterpene measurements were performed with the NOAA PTR-MS instrument (Proton-Transfer-Reaction Mass Spectrometer) on board the NOAA WP-3 aircraft during multiple flights. During TexAQS2000 isoprene was measured using the Innsbruck PTR-MS [*Hawes et al.*, 2003]. A detailed description of the PTR-MS instrument and an intercomparison with gas chromatography (GC) measurements from whole air samples (WAS) can be found elsewhere [*de Gouw and Warneke*, 2007; *de Gouw et al.*, 2006]. During the flights, isoprene, MVK + MACR, and monoterpenes were measured for 1 s each every 17 s. The PTR-MS was calibrated for many VOCs between the flights using a standard mixture containing 500 ppbv of each compound that was diluted to single-ppbv levels. The calibration uncertainty is estimated to be less than 15% for isoprene. PTR-MS measures only the sum of the monoterpenes and therefore the calibration is less certain and depends on the mixture of the individual monoterpenes, and the calibration uncertainty is estimated to be less than 30%. The detection
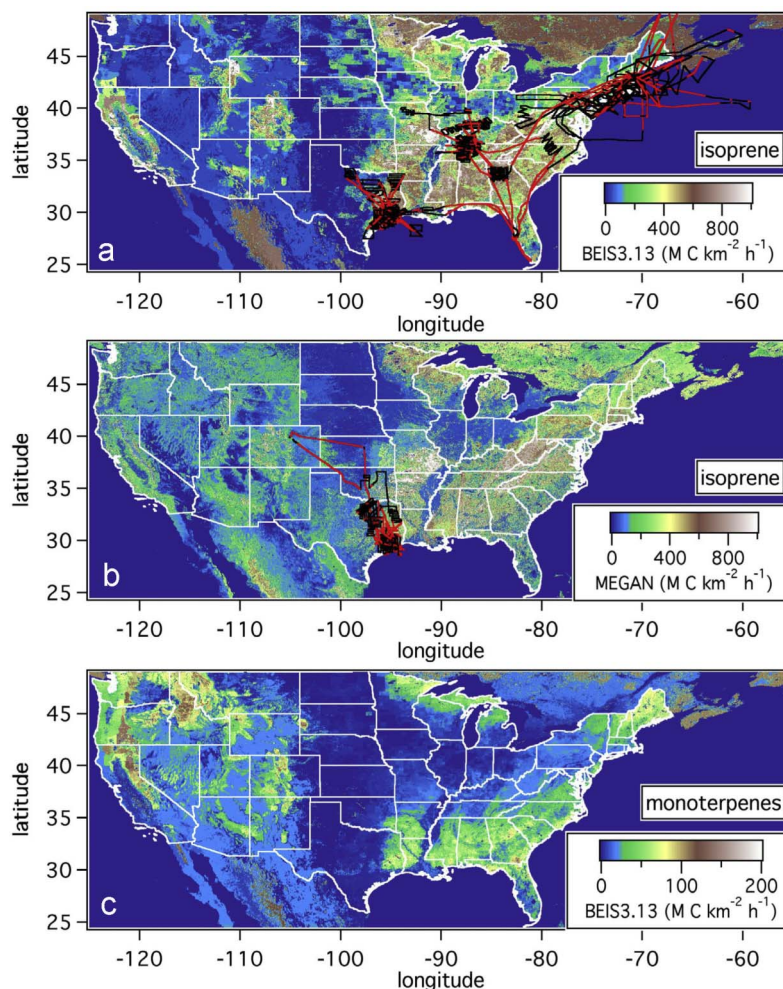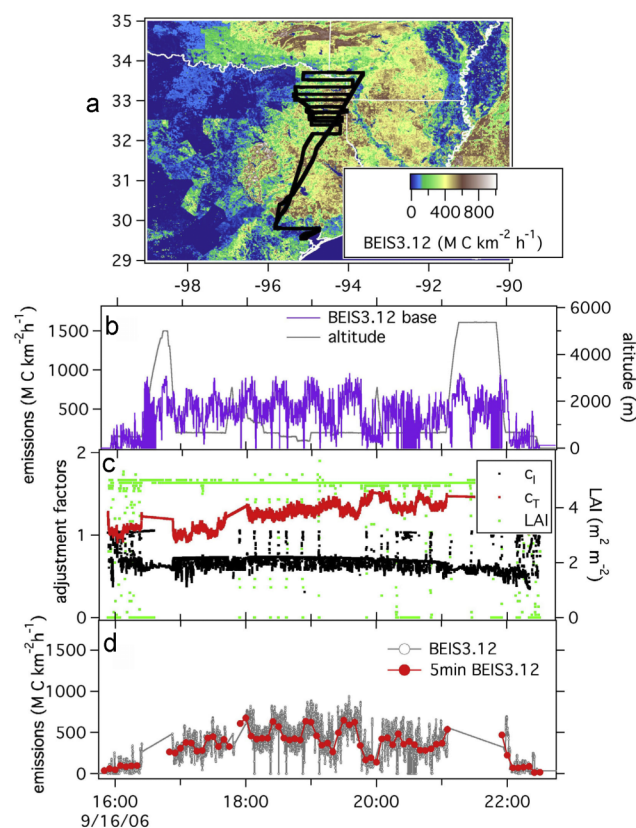
Figure 1. (a) The flight tracks of the NOAA WP-3 aircraft during the NOAA TexAQS2006, ICARTT2004, and SOS1999 campaigns (boundary layer in black and free troposphere in red) plotted on top of the EPA BEIS3.13 summer isoprene base emissions map of the United States. (b) The MEGAN2 isoprene emission factor map with the TexAQS2000 flight tracks. (c) The BEIS3.13 monoterpene base emissions. The units of the emissions here and in the rest of the manuscript are moles C km^{-2} h^{-1}, and the same color scale for the base emissions is used in Figures 2, 4, 9, 10, and 12–15.

limit of the PTR-MS for isoprene and the monoterpenes is about 40 pptv for a 5 s measurement [*de Gouw et al.*, 2003] and was about 70 pptv for a 1 s measurement and about 20 pptv for 5 min averages. In the Houston ship channel, an area close to Houston with a large number of petrochemical facilities, large amounts of anthropogenic VOCs, including isoprene, are released and interferences from species other than isoprene are possible. Interferences for mass 69, on which mass isoprene is detected, have been studied by combining PTR-MS with a gas chromatographic preseparation method [*Warneke et al.*, 2003] and include compounds like cyclopentene, pentanal, and 2-methyl-3-buten-2-ol (MBO). In some isolated plumes near the Houston ship channel, the isoprene measurements have to be taken as an upper limit, but everywhere else the PTR-MS measurements agree well with the GC analysis of the WAS and are therefore assumed to be exclusively isoprene. The scatterplot between the PTR-MS and WAS data using all data from the mission gives a slope of 0.97 and a correlation coefficient of R = 0.70 for TexAQS2006 and a slope of 0.89 and

R = 0.92 for ICARTT2004 [*de Gouw and Warneke*, 2007]. The different measurement frequencies of the two instruments cause a low correlation coefficient for the TexAQS2006 data, because of the higher variability of the isoprene mixing ratios in Texas compared to New England. The Innsbruck PTR-MS used during TexAQS2000 measured isoprene for 2–5 s every 2–40 s (integrations times varied per flight or flight segment). Calibrations were done with a dynamically diluted VOC standard with an estimated accuracy of 20% [*Hawes et al.*, 2003]. Here we use the PTR-MS data instead of the WAS data for TexAQS2000, TexAQS2006 and ICARTT2004, because of the higher time resolution.

[9] During SOS99 isoprene was measured using an airborne gas chromatograph with a flame ionization detector (GC-FID). A 350 cm^3 STP sample was cryogenically acquired for 5 min every 15 min and analyzed in the remaining 10 min. The analytical column was a 30 m × 0.53 mm KCl washed Al$_2$O$_3$ (Chrompack Inc.). A calibrated whole air standard was sampled before, during and after

Figure 2. (a) The flight track of the NOAA WP-3 from the TexAQS2006 flight on 16 September 2006 on top of the BEIS3.12 isoprene base emissions. (b) The base emissions extracted along the flight track together with the aircraft altitude. (c) The light and temperature adjustment factors calculated as described in Appendix A. (d) The actual isoprene emissions from BEIS3.12 along the flight track in the boundary layer as 1 s and 5 min data. The time is in UTC here and for Figures 4 and 7–10.

the flight for calibration. The detection limit was between 2 pptv and 5 pptv for all compounds. More details on the instrument can be found elsewhere [*Goldan et al.*, 2000].

[10] Shortwave solar radiation (200–4700 nm), needed as input for BEIS and MEGAN2, was measured using a standard pyranometer during SOS99 and TexAQS2000 and estimated using data from an actinic flux spectrometer during ICARTT2004 and TexAQS2006 [*Stark et al.*, 2007]. The j_{NO2} data from ICARTT2004 and TexAQS2006 and the slope of j_{NO2} versus shortwave solar radiation from SOS99 and TexAQS2000 were used to estimate the shortwave radiation for ICARTT2004 and TexAQS2006.

[11] Sulfuric acid (H_2SO_4) was measured during ICARTT2004 and TexAQS2006 using a chemical ionization mass spectrometer (CIMS) [*Edwards et al.*, 2003; *Tanner et al.*, 1997]. The uncertainty in the sulfuric acid measurement is about 40%.

[12] Sulfur dioxide (SO_2) was measured by pulsed UV fluorescence [*Ryerson et al.*, 1998] with a detection limit on the order of a few hundred pptv. The uncertainty of the measurement is 10% or ±0.3 ppbv.

[13] Nitrogen dioxide (NO_2) was measured by UV photolysis followed by ozone induced chemiluminescence with a 9% uncertainty [*Ryerson et al.*, 2000].

[14] Particle size distributions and surface were measured with a combination of various condensation particle counters (CPC) and optical particle counters (OPCs) [*Brock et al.*, 2008].

3. Isoprene Emissions Estimated With Emission Models

3.1. EPA BEIS3.12 and EPA BEIS3.13

[15] The most commonly used biogenic emission inventory for the United States is BEIS3, which is publicly available at http://www.epa.gov/asmdnerl/biogen.html. BEIS was first developed in 1988 [*Pierce and Waldruff*, 1991], and updated in the mid 1990s to BEIS2 [*Pierce et al.*, 1998]. Those previous versions and the latest version, BEIS3, estimate volatile organic compound (VOC) emissions from vegetation and nitric oxide (NO) emissions from soils. In this paper we use the two latest versions, BEIS3.12 and BEIS3.13. Both include a 1 km vegetation database that resolves forest canopy coverage by tree species, and emission factors for 34 chemicals including isoprene, 14 monoterpenes and methanol. Changes from version BEIS3.12 to BEIS3.13 include very small updates in the base emission factors for isoprene and a slight increase in monoterpenes in the northeastern United States and small decreases in the northwestern United States. The light adjustment factor changed more significantly between the two versions, as will be discussed in detail below. On average the change resulted in a decrease of 35% in isoprene and 2% in monoterpene emissions. The BEIS3.13 summer isoprene and BEIS3.13 monoterpene base emissions are shown in Figure 1.

[16] To calculate the actual isoprene emissions from BEIS3, the base emissions have to be multiplied with the temperature and light adjustment factors to account for environmental dependence of the isoprene emissions [*Guenther et al.*, 1995].

$$\text{actual emission} = \text{base emission} \times c_T \times c_L, \qquad (1)$$

where c_T is the temperature adjustment factor and c_L is the light adjustment factor.

[17] In this work, we extracted the base emissions and leaf area index (LAI), needed for the calculation of c_L, provided together with BEIS3, along the flight tracks, and all other necessary parameters (shortwave radiation, zenith angle, ground temperature and pressure) were determined from the actual aircraft measurements. For the analysis presented here, c_T and c_L are determined along the flight track using the same formalism as used in the BEIS3.12 and BEIS3.13 emission modules in the WRF-Chem air quality forecast model [e.g., *McKeen et al.*, 2005]. The major update from BEIS3.12 to BEIS3.13 is a difference in the calculation of c_L, which causes a reduction in the isoprene emission from version 3.12 to 3.13. In Appendix A the calculation of c_T and c_L using aircraft data is described in detail.

[18] An example of extracting the isoprene emissions from BEIS3.12 along the flight tracks is shown in Figure 2.
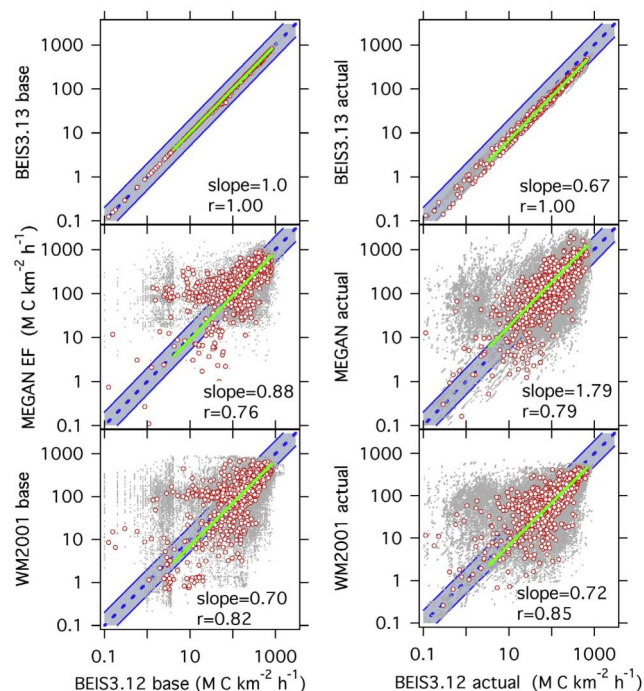
Figure 3. Scatterplots of the isoprene base and actual emissions in BEIS3.13, MEGAN2, and WM2001 versus BEIS3.12. The gray dots are the 1 s data, and the red circles are the 5 min averages. The blue shaded areas indicate an agreement to within a factor of 2, and the solid green line is an orthogonal distance regression fit forced through zero of the 5 min average data.

On 16 September 2006 the NOAA WP-3 flew over a densely forested area in northeast Texas; the flight track is shown on top of the BEIS3.12 base emissions map. The base emissions are extracted along the flight track and are shown in Figure 2b. LAI is also extracted and shown in Figure 2c together with the isoprene emission adjustment factors c_L and c_T, calculated according to the description in Appendix A. The LAI is generally around 5 m^2 m^{-2} in northeast Texas, only a small number of points with low LAI values were found and are attributable to rivers, lakes and the Houston ship channel resulting in higher values of c_L due to assumed less shading of the lower leaves. The base emissions at these locations are also low, and this small number of points does not significantly influence the analysis here. The warm temperatures in Texas during summer result in large values for c_T (>1) and in potentially large emission. Using all those parameters, the actual emissions are calculated according to equation (1) and plotted in Figure 2d. The 1 s data are shown together with 5 min averages along the flight track.

[19] The scatterplots of the base and actual emissions calculated using BEIS3.13 versus BEIS3.12 for all data from the TexAQS2006 campaign are shown in Figure 3. The base emissions are almost identical. The major difference is in the light adjustment factor resulting in about 30% lower actual emissions in BEIS3.13. A linear fit was made to the 5 min data using an orthogonal distance regression fit forced through zero. This type of fit was done for all scatterplots in this analysis. The correlation coefficient, R,

is 1.00. The results from the three other campaigns are similar and are therefore not shown here.

3.2. MEGAN2

[20] MEGAN2 is a biogenic emissions model that was recently introduced by *Guenther et al.* [2006]. It is a global-scale model with a base resolution of $\sim$1 km^2 (30 s latitude by 30 s longitude) to enable both regional and global model simulations. Isoprene and other trace gases and aerosol emissions at every location are estimated by

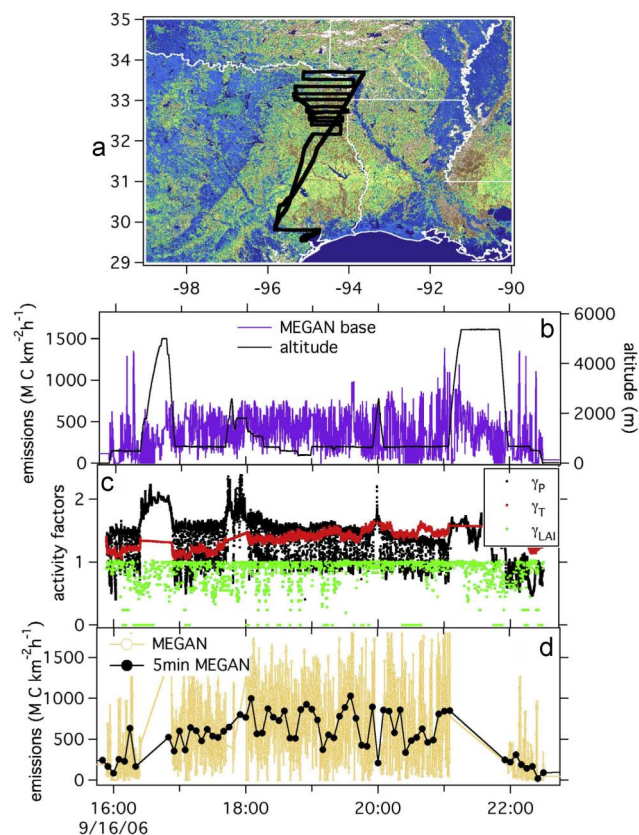$$\text{Emission} = [\varepsilon][\gamma][\rho], \qquad (2)$$

where ε is an emission factor for a compound at standard conditions (30°C and 1000 μmol m^{-2} s^{-1} PAR), γ is an emissions activity factor that accounts for emission changes due to deviations from standard conditions as is discussed in detail in Appendix B, and ρ is a factor that accounts for loss within the canopy. We have used MEGAN code version 2.04 and emission factor version 2.0 in this manuscript. The MEGAN2 emission factor map is shown in Figure 1b. Some regional differences between MEGAN2 and BEIS3.13 base emissions are obvious and will be discussed below.

[21] The calculation of the actual isoprene emissions from MEGAN2 for the example flight on 16 September 2006 in northeast Texas is shown in Figure 4. The emission factor map is shown together with the flight track in Figure 4b. The emission factor is extracted along the flight track and shown in Figure 4b. It is seen that the MEGAN2 emission factor map has more spatial variability in this area than BEIS3.12 shown in Figure 2b. A detailed description of how the emission activity factors are calculated using measured data on the aircraft is given in Appendix B. The temperature, light and LAI emission activity factors, using the MEGAN2 2003 LAI data, for this flight are shown in Figure 4c and the resulting actual isoprene emissions in Figure 4d. The 1 s data and 5 min averages are shown.

[22] The scatterplots of the base and actual MEGAN2 emissions versus BEIS3.12 for all data from the Tex-AQS2006 campaign are shown in Figure 3. A linear fit was made to the 5 min data using an orthogonal distance regression fit forced through zero. The base emission factors in BEIS3.12 and MEGAN2 are not directly comparable. In BEIS3.12 the base emissions are the emissions expected if all leaves in a canopy were exposed to 1000 μmol m^{-2} h^{-1} while in MEGAN2 the base emission factor is the emission expected if the light at the top of the canopy is 1500 μmol m^{-2} h^{-1}. The difference in base emissions of about 10% is therefore not meaningful, but clear regional differences exist, resulting in a lower correlation coefficient of R = 0.76. The actual emissions from MEGAN2 are 80% higher than BEIS3.12 as a result of the higher light emission activity factor. The same amount of scatter exists as for the base emissions. The comparisons for the three other campaigns yield similar results and are therefore not shown here.

3.3. Wiedinmyer 2001

[23] For Texas only, a third isoprene emission model was used to compare with the measurement data. This model was developed by *Wiedinmyer et al.* [2001] and will be

Figure 4. (a) The flight track of the NOAA WP-3 from the TexAQS2006 flight on 16 September 2006 on top of the MEGAN2 isoprene base emission factor. (b) The base emissions extracted along the flight track together with the aircraft altitude. (c) The light, temperature and LAI adjustment factors calculated as described in Appendix B. (d) The actual isoprene emissions from MEGAN2 as 1 s and 5 min data.

called WM2001 in the remainder of this manuscript. Using data from a variety of sources, the land use and vegetation in Texas were mapped with a spatial resolution of approximately 4 km. Over 600 classifications were used to characterize the land use and land cover throughout the state and field surveys were performed to assign leaf biomass densities by species to the land cover classifications. The land cover data were used as input to a biogenic emission model, GLOBEIS2. Estimates of biogenic emissions of isoprene based on GLOBEIS2 and the new land cover data showed significant differences when compared to biogenic isoprene emissions estimated using previous land cover data and emission estimation procedures [*Wiedinmyer et al.*, 2001].

[24] The light and temperature dependence for the WM2001 isoprene emission model are the same as in BEIS3.12 as described in Appendix A. The scatterplot of the base and actual emissions of WM2001 versus BEIS3.12 are shown in Figure 3. The base emissions are about 30% lower in WM2001 than in BEIS3.12 and some regional differences exist that result in a correlation coefficient of R = 0.82. The actual emissions from WM2001 calculated

with the BEIS3.12 light dependence are therefore about 30% lower in WM2001 than in BEIS3.12 as shown in Figure 3.

4. Isoprene Emissions Estimated From the Aircraft Measurements

[25] The isoprene emission flux along the flight tracks in the boundary layer can be modeled from the measured mixing ratio using a simple mixed boundary layer approach that takes the boundary layer height and the isoprene lifetime into account. The emissions can be estimated by

$$Emissions_{isoprene} - F_e = [isoprene] * BL_{height} * k_{OH} * [OH], \quad (3)$$

where [isoprene] is the measured concentration, BL_{height} the observed boundary layer height, k_{OH} the rate coefficients with OH, and [OH] the OH concentrations. This approach neglects horizontal advection. F_e is the entrainment flux from the boundary layer into the free troposphere. The term $k_{OH}*[OH]$ represents the inverse lifetime of isoprene due to reaction with OH (k_{OH} is 101×10^{-12} cm^3 molecule^{-1} s^{-1} [*Atkinson et al.*, 2005]). The entrainment flux out of the boundary is estimated to be 30% of the emission flux as was recently found for isoprene flux measurements from an aircraft over the Amazonian rain forest [*Karl et al.*, 2007] using the mixed layer gradient method. This might not be representative for the forest in the United States and could therefore contribute to the error in this calculation as discussed below.

[26] The boundary layer height was quantitatively determined for each profile flown by the WP-3 aircraft by looking at the isoprene, potential temperature and water vapor altitude profiles. Generally the observed daytime boundary layer heights for all three campaigns were between 1500 m and 2000 m as can be expected for the continental United States during summer. As expected, lower values were encountered during nighttime flights and tracks over the ocean. An altitude profile of isoprene from the TexAQS2006 flight on 16 September 2006 in northeast Texas is shown in Figure 5. All the data from this flight are shown; highlighted is the part of the flight that was a stair step profile over the same east-west track (1750 until 1900 UTC in Figures 2 and 4). The average boundary layer height for this flight was determined to be 1.4 km, which was lower than most other flights. For each flight an average boundary layer height was used, because profiles were flown too infrequently during each flight to describe the time evolution of the boundary layer. The altitude profile also shows the variation in the boundary layer height and the transition from the boundary layer to the free troposphere, which is between 1.2 km and 1.5 km. This flight was rather unusual; during most other flights the boundary layer height was larger (about 2 km) and the transition sharper. Figure 5 also demonstrates that isoprene was very well mixed throughout the boundary layer, a small decrease was observed that was statistically not significant. A well-mixed boundary layer, as was observed here and almost everywhere during the different field campaigns, is necessary for the calculation of the isoprene emissions using the simple mixed boundary layer approach.
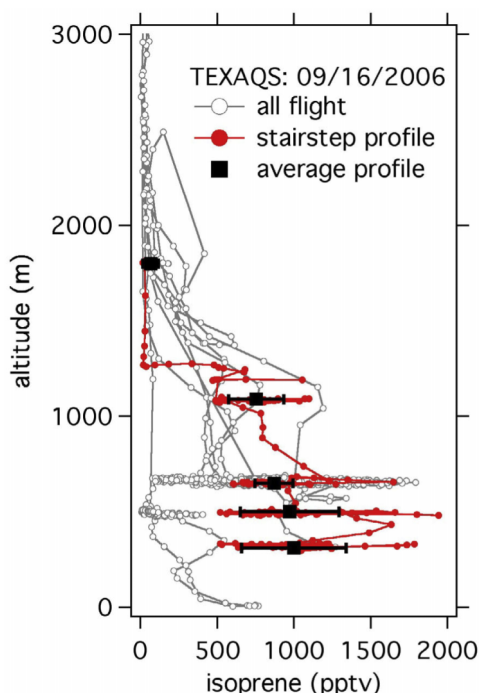
Figure 5. Altitude profile of isoprene from the Tex-AQS2006 flight on 16 September 2006. All the data from the flight are shown in gray, highlighted in red is a stair step profile, and averages for each level flight within the stair step profile are given in black, where the error bars are the standard deviation.

[27] OH was measured only during the ICARTT2004 mission, but the data quality and coverage were very low and instead a parameterization was used to estimate [OH] along the flight tracks [*Ehhalt and Rohrer*, 2000]. The parameterization makes use of photolysis frequency measurements of j_{O^1D} and j_{NO_2} as well as the measured NO_2 concentrations in ppbv,

$$[OH] = a(j_{O^1D})^\alpha (j_{NO_2})^\beta \frac{bNO_2 + 1}{cNO_2^2 + dNO_2 + 1}. \quad (4)$$

[28] The parameterization is based on data obtained in a rural area in northeastern Germany during the POPCORN campaign and accurately reproduced the measured OH values ($R^2 = 0.93$). The parameters of [*Ehhalt and Rohrer*, 2000] are $\alpha = 0.83$, $\beta = 0.19$, a = 4.1×10^9, b = 140, c = 0.41, and d = 1.7, indicating a strong, slightly nonlinear dependence of OH on j_{O^1D} and a small but highly nonlinear contribution from j_{NO_2}. This OH parameterization does not include an influence of isoprene and other VOC changing the OH concentration [e.g., *Lelieveld et al.*, 2008]. The parameterization was used previously in the New England area and compared well (slope = 0.79 and $R^2 = 0.84$) with a detailed calculation of [OH] that considered its sources and sinks [*Warneke et al.*, 2004]. A similar approach reproduced a multiyear [OH] measurement at the Hohenpeissenberg Observatory very well [*Rohrer and Berresheim*, 2006]. This parameterization was determined from ground site measure-

ments and is not applicable to the free troposphere, but boundary layer data only are used here for the determination of the isoprene emission flux.

[29] To evaluate the accuracy of the OH parameterization we have estimated OH by a second, completely independent approach using measured sulfuric acid, SO_2 and aerosol surface area. In the atmosphere, sulfuric acid is formed from the reaction of SO_2 + OH and its primary sink is loss to aerosols. For this reason, H_2SO_4 may be used as a photochemical tracer within the boundary layer to estimate the OH levels. Assuming that H_2SO_4 is irreversibly lost to aerosol scavenging, the average lifetime was 3 min for the ICARTT2004 mission. As a result, the OH concentration can be calculated through a steady state approximation assuming diffusion-limited uptake of H_2SO_4 by the aerosol, $R_{aerosolUptake}$,

$$[OH]_{SS} = \frac{R_{AerosolUptake}}{k[SO_2]}$$
$$R_{AerosolUptake} = \left(\frac{4}{\nu\alpha}\right)^{-1} An_x, \quad (5)$$

where ν is the molecular speed, α is the mass accommodation coefficient, A is the Fuchs surface area, and n_x is $[H_2SO_4]_{(g)}$ [*Jacob*, 2000]. For this analysis, the value of the mass accommodation coefficient used was 0.7 as suggested by *Chen et al.* [2005]. OH concentrations were only calculated for sulfur dioxide concentrations larger than 1 ppbv using equation (5). This filter was applied because of the detection limit of SO_2 on the order of a few hundred pptv. The error in the OH calculation was shown to be smaller than a factor of 2 [*Chen et al.*, 2005]. The H_2SO_4 steady state model calculation will be described in more detail elsewhere (A. T. Hanks et al., manuscript in preparation, 2010). Figure 6 shows a scatterplot of OH calculated using equation (4), the Ehhalt parameterization, versus OH calculated using equation (5), the SO_2 steady
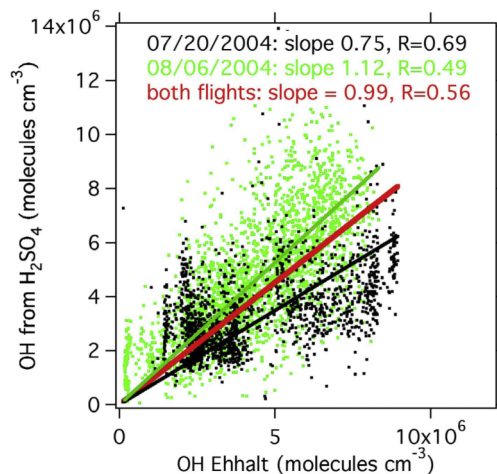
Figure 6. Comparison of OH calculations using the Ehhalt parameterization and the H_2SO_4 steady state model for the ICARTT2004 flights on 20 July 2004 and 6 August 2004. The linear fits for the individual flights are shown in green and black, and the fit through all data is shown in red.
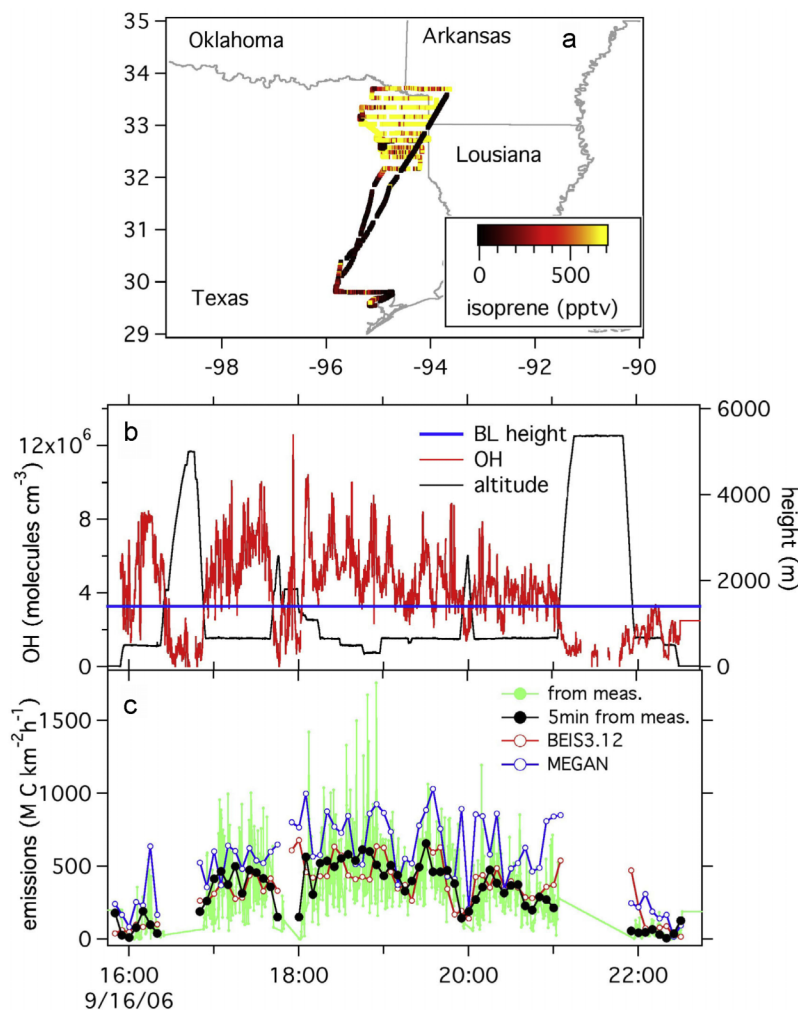
Figure 7. (a) The flight track of the NOAA WP-3 from the TexAQS2006 flight on 16 September 2006 color coded with isoprene mixing ratios. (b) The boundary layer height and the OH concentration used for modeling the emissions from the isoprene observations together with the aircraft altitude. (c) The emissions modeled from the measurements and calculated from BEIS3.12 and MEGAN2.

state model, for two flights during ICARTT2004. Results from only two flights over land are available for the SO_2 steady state model because of the limited availability of H_2SO_4, sufficiently high SO_2 and surface area measurements. The flight on 20 July 2004 took place in New England following the New York City plume over Long Island along the coast to Massachusetts. The flight on 6 August 2004 went from Boston, New York City to the Ohio River Valley and back. The two completely independent methods for estimating OH agree on average within 25%. The Ehhalt parameterization was not tested thoroughly in VOC rich air masses and may not be accurate under such conditions [*Lelieveld et al.*, 2008]. However, the good agreement between average OH estimated from Ehhalt and determined from the H_2SO_4 measurements lends confidence in our OH estimates and also provides a better estimate of the OH uncertainty.

[30] In Figure 7 the parameters needed for the calculation of the emissions from the measurements for the flight on 16 September 2006 are shown. The observed isoprene mixing ratios in the boundary layer along the flight track in Figure 7a were high and highly variable. Figure 7b shows the bound-

ary layer height, which was estimated to be 1.4 km in northeast Texas for this flight, together with the OH concentration calculated according to equation (4) using the Ehhalt parameterization. Maximum OH values for this flight were around 1×10^7 molecules cm^{-3}.

[31] The emissions calculated from the mixing ratios are shown in Figure 7c as 1 s data and 5 min averages together with the emissions calculated from BEIS3.12 and MEGAN2 as illustrated in Figures 2 and 3. It is seen that on average the emissions estimates from the measurements agree well with those estimated from BEIS3.12, but that the emissions from MEGAN2 are somewhat higher. It should be noted that in this region the emission estimates from MEGAN2 were highly variable. Looking at the BEIS3.12 and MEGAN2 base emissions, the high variability is also evident. In areas like this, a point-by-point comparison on a 1 s time base (or 1 km grid), although possible with this data set, is not extremely meaningful because of the horizontal advection. Five minute averages, on the other hand, can be compared well.

[32] The following uncertainties contribute to the total error for this method.

[33] 1. The accuracy of the isoprene measurement is about 15%.

[34] 2. Boundary layer heights were estimated using measured profiles of potential temperature, humidity and isoprene made during profiles. Differences between multiple profiles during the same flight indicate that there is a ~10% uncertainty in this estimate.

[35] 3. The OH used in this analysis is determined from a parameterization and for some flights from a steady state model using the H_2SO_4 measurements. The two independent methods of determining OH agree within 25%, but point-by-point differences are sometimes up to a factor of 2. Both methods have an estimated error of at least 50% and we therefore assume a significant error from the use of the OH calculation of at least 50%.

[36] 4. This method estimates the emissions along the flight track by taking the isoprene lifetime into account, but does not consider horizontal transport. As will be discussed in more detail later, isoprene was frequently observed out over the ocean in New England after transport from the forested regions around Boston, even though emissions over the ocean are zero in the inventories. The method described here will incorrectly attribute this transported isoprene to emissions from the ocean. This effect will cause a random error and therefore might not strongly influence the magnitude of the emissions over a large area.

[37] 5. Looking at the altitude profiles flown, no systematic altitude dependence was observed that indicates incomplete vertical mixing throughout the boundary layer, but there will be locations where incomplete mixing will cause an error in the determination of the emissions.

[38] 6. Another large error involves the entrainment flux from the boundary layer. Here a constant flux of 30% from the emissions was used [*Karl et al.*, 2007]. The entrainment flux certainly will not be a constant fraction of the emissions and will be larger or smaller than the 30% in different areas and time of day.

[39] We conclude that the overall uncertainty in estimating the emissions from the measurements is a factor of 2 (−50%, +100%). The uncertainties in the calculation of the emissions from the inventories are small in comparison. They include measurement uncertainties in the shortwave radiation, influence of cloud cover on the surface radiation, and errors in determining the ground temperature from aircraft measurements, but are assumed to be less than 10%. This does not mean that the emission inventories are accurate to within 10%: the error estimate assumes that the base emissions and the canopy environment models are correct. Taking all the estimated errors into account, the different emission estimates shown in Figure 7c for the 16 September 2006 flight in Texas agree within the estimated uncertainties on average.

5. Isoprene Mixing Ratios Estimated With FLEXPART Transport Model

5.1. FLEXPART Transport Model

[40] The FLEXPART Lagrangian particle dispersion model [*Stohl et al.*, 2005] was used to simulate isoprene and monoterpene mixing ratios during ICARTT2004 and TexAQS2006. FLEXPART was driven by model-level data from the European Centre for Medium-Range Weather

Forecasts (ECMWF) with a temporal resolution of 3 h and 91 vertical levels and a horizontal resolution of $0.36° \times 0.36°$. FLEXPART parameterizes turbulence in the boundary layer and in the free troposphere by solving Langevin equations [*Stohl and Thomson*, 1999]. Isoprene emissions were taken from BEIS3.12 with a resolution of $0.3° \times 0.3°$ for ICARTT2004 and $0.15° \times 0.15°$ for TexAQS2006. The temperature and light dependence of isoprene was calculated hourly for each isoprene emission grid with the canopy environment model as described in Appendices A1 and A2. ECMWF 2 m above ground temperature and net solar radiation were used for this purpose and interpolated linearly in space and time using the two nearest ECMWF fields. The same canopy environment model was used in Appendix A with measured data.

[41] FLEXPART backward calculations were used to calculate the isoprene mixing ratios along the flight tracks. In the backward mode, sets of 6500 particles are fitted into boxes placed along the aircraft pathway with a vertical size of 250 m and a horizontal size of $0.1° \times 0.1°$. Retroplumes were initialized by releasing particles uniformly over 10 min time intervals. The sensitivity function to surface emission of the particles is recorded each hour within a layer between the surface and 50 m above the ground (the so-called footprint layer), and in an output grid with the same resolution of the calculated isoprene surface emission. FLEXPART has been used so far for long-lived tracers such as CO and transport over many days is simulated. Here we use a short-lived tracer for the first time in FLEXPART and much shorter timescales have to be considered. Isoprene is approximated in FLEXPART by accumulating all surface emissions to which a Lagrangian parcel has been exposed over the previous 1 h. The FLEXPART tracer that takes transport and emissions over the last hour into account was used to compare to the isoprene and monoterpene measurements, tracers with longer times will be used to compare to isoprene plus its oxidation products and for nighttime flights.

5.2. Calculation of Isoprene Mixing Ratios With FLEXPART

[42] Figure 8 illustrates the way FLEXPART is used to calculate the isoprene mixing ratio along the flight track. In Figure 8a the footprint calculated with FLEXPART for one point along the flight track during the 16 September 2006 flight is shown. The footprint is multiplied with the isoprene emissions at each location to calculate the mixing ratio. The aircraft takes about a minute to move through each box that is used to release the FLEXPART particles and the same isoprene mixing ratio is prescribed for all data points within this box to generate 1 s data along the flight tracks. The model time step used is 15 min, but we calculate the residence time of the particles in grid cells hourly. For isoprene we look at transport times of 1 h, which is only a very small region around the star that indicates the aircraft location. The character 1 along the footprint indicates roughly one day of transport. The model uses temperature and PAR from the ECMWF meteorology to determine actual emissions from the base emissions.

[43] Figure 8b demonstrates which grid cells contribute to the overall residence time at the surface for one point along the flight track. The NOAA P3 aircraft was flying most of
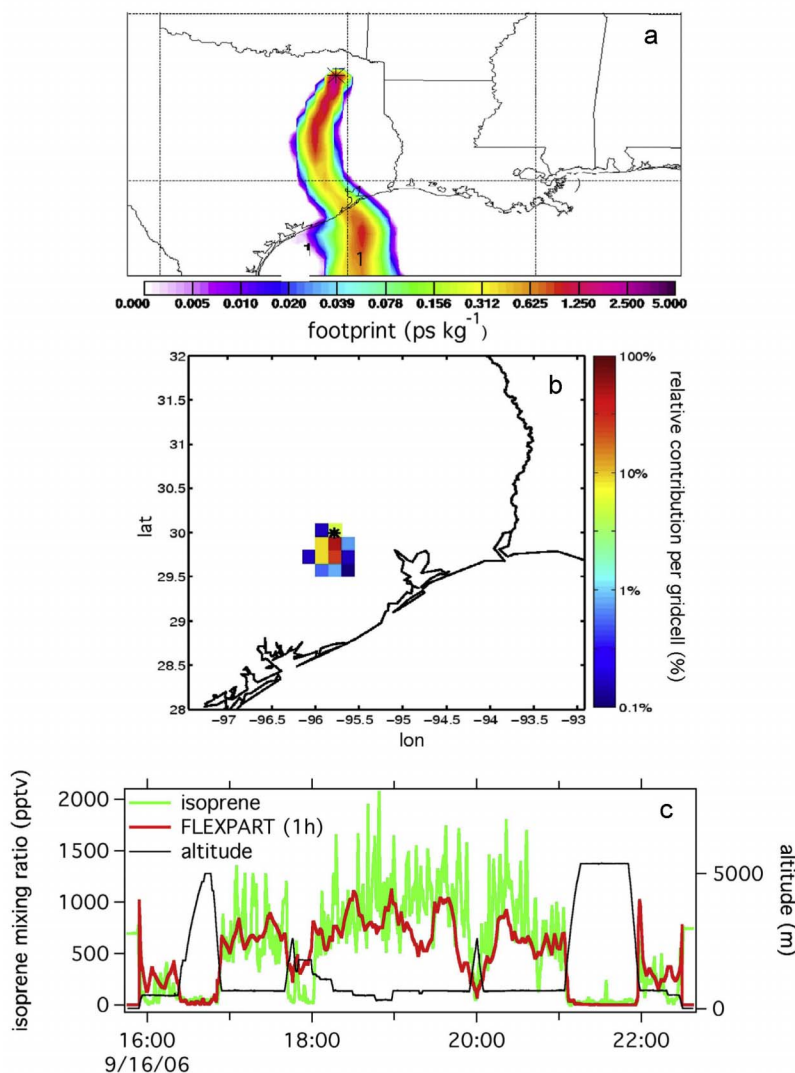
Figure 8. (a) Footprint calculated with FLEXPART for one representative point along the flight track on 16 September 2006. The aircraft altitude for this point was 500 m. The character "1" in the footprint plot indicates the average location after 1 day of transport of all the particle back trajectories calculated from the aircraft location. The footprint is multiplied with the isoprene emissions at each location to calculate the mixing ratio. (b) Relative contribution on the overall residence time at the surface per grid cell within 1 h of transport calculated with FLEXPART. The location of the aircraft is given with the star, which is just north of Houston, Texas. (c) Time series of measured isoprene is in green, and calculated with FLEXPART using emissions within 1 h of transport is in red.

the time above 500 m in altitude and to get a large contribution from the grid cell above which the aircraft is located, one needs an average wind speed of less than 15 km/h However, the highest contribution is generally found in one of the nearest grid cells. The contribution from each grid cell to the isoprene mixing ratio calculated from FLEXPART then further depends on the actual isoprene emissions in this grid cell.

[44] In Figure 8c the measured isoprene mixing ratio is shown together with the FLEXPART model results for this flight. The FLEXPART data shown here are the 1 h tracer. The observed isoprene mixing ratios were extremely variable during this flight and the model does not capture this small-scale variability, but the main features and the mag-

nitude are described well. This analysis is not restricted to boundary layer data but although the free troposphere data can be compared as well, they are basically zero in the FLEXPART calculation. The regression slopes presented below are almost identical for the data with or without the free troposphere. It should be mentioned here that an isoprene spike was observed at high altitude around 2130 UTC during this flight, which was caused by rapid vertical transport in a convective cloud system, as shown by other tracers measured onboard the aircraft.

[45] The following uncertainties contribute to the total error for this method.

[46] 1. The main uncertainty in this method is caused by the short lifetime of isoprene during the day compared to the
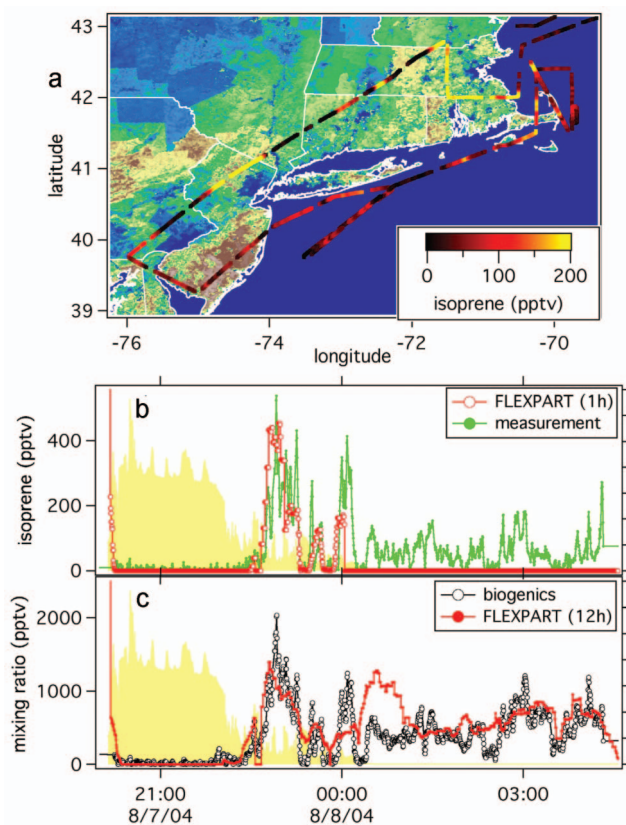
Figure 9. (a) The flight track of the NOAA WP-3 from the ICARTT2004 flight on 7 August 2004 color coded by the measured isoprene mixing ratio on the BEIS3.12 base emissions map. Elevated isoprene was found on flight segments over the ocean. (b) Measured isoprene mixing ratios and calculated from FLEXPART using transport times within 1 h. The yellow shaded area indicates the measured shortwave radiation. (c) Time series of biogenics (= isoprene+1.66*[MVK+MACR]) together with FLEXPART calculations of isoprene using emissions and 12 h of transport.

model time steps. In Figure 7 the OH concentration for a flight in Texas ($3-8 \times 10^6$ molecules cm^{-3}) can be seen. The resulting isoprene lifetime is therefore around $0.5-1$ h, which was typical for all other daytime flights as well. During ICARTT2004 the lifetimes were usually somewhat longer, closer to 1 h, due to differences in photochemistry and latitude from the northeast UNITED STATES compared to Texas. A considerable amount of isoprene will be lost during the 1 h of transport, causing a possible overestimation of the mixing ratios. On the other hand, isoprene emitted at the end of the day, when the lifetime is long, will be still present during the night, if NO$_3$ chemistry is slow as discussed below. This effect causes an underestimation of the mixing ratios by FLEXPART.

[47] 2. Model uncertainties involve the errors in the 2 m above ground temperature and net solar radiation used for determining the isoprene emissions from BEIS3.12. The net solar radiation may be an overestimate or underestimate depending on how well the ECMWF calculates the cloud cover. Furthermore, the precision of the backward trajectories is affected by the precision of the ECMWF wind fields

in the boundary layer, and the fact that the wind fields are linearly interpolated at each time step in the model (each 7.5 min) between the two nearest ECMWF fields.

[48] We conclude that the overall uncertainty of this method is approximately a factor of 2 (-50%, $+100\%$) and therefore the model results shown in Figure 8c agree with the observations within the uncertainties.

5.3. Isoprene Transport

[49] During the day isoprene has a short lifetime of $0.5-1$ h at most due to OH reactions and therefore will not be transported over large distances. Isoprene emitted at the end of the day is exposed to much lower OH and is only oxidized significantly if NO$_3$ is present, but often will be transported over larger distances [*Brown et al.*, 2005]. One example is shown in Figure 9, which shows a flight track of the NOAA WP-3 during the ICARTT2004 campaign. The flight started on 7 August 2004 and went into the early morning of 8 August 2004. The flight track in the top panel is color coded by the measured isoprene mixing ratios and is shown on top of the BEIS3.12 isoprene base emissions map. Significant parts of this flight were over water, but even in those areas elevated mixing ratios of transported isoprene were encountered. The time series of isoprene and the FLEXPART 1 h tracer are shown in the Figure 9b. Also shown is the shortwave radiation with the yellow shaded area to indicate when the night starts and the isoprene-OH chemistry stops. During the second part of the flight, which was mainly over water, up to 200 pptv of isoprene were found. FLEXPART indicates zero, which means that there were no emissions within the last hour. FLEXPART tracers with longer times for transport and emissions can be used here to compare to the measurements. The FLEXPART 12 h tracer is shown in Figure 9c. For transport over many hours the isoprene chemistry can no longer be neglected and all the oxidation products of isoprene have to be added to the isoprene mixing ratio. The sum of methyl vinyl ketone (MVK) and methacrolein (MACR) was also measured with the PTR-MS during this flight. MVK and MACR are significantly longer lived than isoprene during day and night: k$_{OH}$ is 33×10^{-12} cm^3 molecule^{-1} s^{-1} and k$_{NO3}$ is 0.0033×10^{-12} cm^3 molecule^{-1} s^{-1} for MACR and k$_{OH}$ is 19×10^{-12} cm^3 molecule^{-1} s^{-1} and k$_{NO3}$ is 0.0006×10^{-12} cm^3 molecule^{-1} s^{-1} for MVK [*Atkinson et al.*, 2006]. Together they have a yield of about 60% [*Atkinson et al.*, 2006], which can be used to roughly estimate the isoprene mixing ratio at the time of emission as described by [*de Gouw et al.*, 2005]:

$$\text{biogenics} = \text{isoprene} + 1.66 \times (\text{MVK} + \text{MACR}). \quad (6)$$

[50] The biogenics signal is shown in Figure 9c and it can be seen that it reproduces the observed biogenics over the ocean well with the 12 h FLEXPART tracer for this flight clearly indicating that isoprene was transported over long distances during the evening and the night.

6. Monoterpenes

[51] Measurements of the sum of the monoterpenes are available for the ICARTT2004 and TexAQS2006 campaigns. The largest observed mixing ratios during both
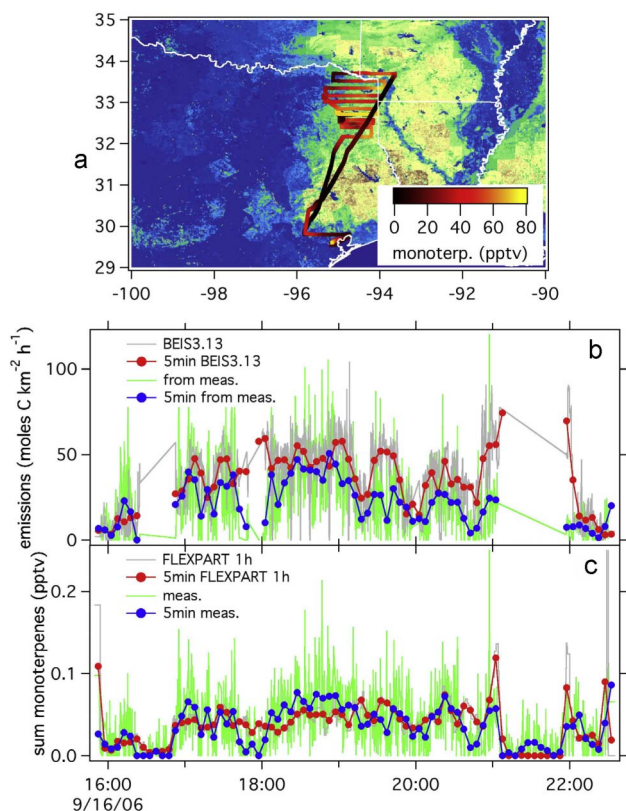
Figure 10. (a) The flight track of the NOAA WP-3 from the TexAQS2006 flight on 16 September 2006 color coded with monoterpene mixing ratios on top of the BEIS3.13 monoterpene base emissions. (b) The emissions modeled from the observation and from BEIS3.13. (c) The measured mixing ratios and the ones calculated using FLEXPART with emissions within 1 h.

campaigns were below 100 pptv, which is close to the detection limit of PTR-MS and introduces significant uncertainties in the analysis. The emissions modeled from the observations are determined in the same way as described for isoprene earlier and are calculated as follows:

$$
\begin{aligned}
\text{Emissions}_{\text{monoterpenes}} - F_e = & \, [\text{monoterpenes}] \times \text{BL}_{\text{height}} \\
& \times (k_{OH} \times [OH] + k_{O_3} \times [O_3]).
\end{aligned} \tag{7}
$$

Table 1. Slopes and Correlation Coefficients R for Linear Fits of Scatterplots for the Isoprene Emissions Determined From the Biogenic Emission Inventories Versus the Emissions Modeled From the Measurements Using the Mixed Boundary Layer Method[a]

	BEIS3.12 Isoprene	BEIS3.13 Isoprene	MEGAN2 Isoprene	WM2001 Isoprene
SOS1999	0.61 (0.73)	0.43 (0.75)	1.09 (0.59)	N/A
TexAQS2000	0.47 (0.62)	0.34 (0.64)	1.30 (0.68)	0.50 (0.52)
ICARTT2004	1.65 (0.66)	0.98 (0.67)	2.83 (0.68)	N/A
TexAQS2006	0.98 (0.69)	0.60 (0.63)	1.81 (0.63)	0.68 (0.73)

[a]Correlation coefficients R are given in brackets. Values above 1 imply that the inventories are larger. The linear fit is an orthogonal distance regression forced through zero.

[52] For the monoterpenes, we also take the loss due to ozone into account. The k_{OH} and k_{O_3} are the rate coefficients with OH and ozone, respectively, and [OH] and [O$_3$] the OH and ozone concentrations. F_e is the entrainment flux from the boundary layer into the free troposphere and was also estimated to be 30% of the emission flux. The lifetime of the sum of the monoterpenes was estimated using a k_{OH} of 80×10^{-12} cm^{-3} molecule^{-1} s^{-1} and k_{O_3} of 4×10^{-17} cm^{-3} molecule^{-1} s^{-1}, based on an average monoterpene mix [*Geron et al.*, 2000]. The lifetime during the day is a little longer than for isoprene at 0.5–1 h in Texas and about 1 h in the northeast. The emissions along the flight track from BEIS3.13 are calculated according to Appendix A. Total monoterpenes were incorporated into FLEXPART using BEIS3.13 and mixing ratios were calculated along the flight tracks for emissions within the last hour of transport. The uncertainties involved are the same as for isoprene; only the measurement uncertainty for the monoterpenes is larger than for isoprene.

[53] Figure 10 shows the flight track of the 16 September 2006 flight in Texas on top of the BEIS3.13 base emission map color-coded with the measured monoterpene mixing ratio. Figure 10a shows the emissions determined from BEIS3.13 and modeled from the observations and Figure 10b the measured mixing ratio and the result of the FLEXPART calculation. The results for both methods agree quite well for this flight. This was the flight with the highest observed mixing ratios during both campaigns; the measurements and inventories agreed less well for flights with lower mixing ratios.

7. Results and Discussion
7.1. Quantitative Comparison

[54] For each campaign we made scatterplots of the emissions of isoprene and monoterpenes estimated from the measurements versus the emissions calculated from the different inventories in the same way as shown in Figure 3. Furthermore the mixing ratios calculated with FLEXPART were plotted versus the measured mixing ratios. The slopes and the correlation coefficients of all the linear fits are given in Tables 1, 2, and 3 and Figure 11. The 5 min averages were used and the linear fit was an orthogonal distance regression forced through zero.

[55] For the scatterplots all the data from the respective campaigns were used, including nighttime data. The isoprene emissions calculated both from the inventories (due to the light dependence) and from the measurements (due to OH being small) are zero at night. Monoterpene emissions

Table 2. Slopes and Correlation Coefficients R for Linear Fits of Scatterplots for the Mixing Ratios Calculated With FLEXPART Versus Measured Mixing Ratios[a]

	FLEXPART Isoprene
SOS1999	N/A
TexAQS2000	N/A
ICARTT2004	2.05 (0.61)
TexAQS2006	1.30 (0.75)

[a]Correlation coefficients R are given in parentheses. Values above 1 imply that the inventories are larger. The linear fit is an orthogonal distance regression forced through zero. N/A denotes not available.

Table 3. Slopes and Correlation Coefficients R for Linear Fits of Scatterplots for the Monoterpene Emissions Determined From the Biogenic Emission Inventories Versus the Emissions Modeled From the Measurements Using the Mixed Boundary Layer Method[a]

	BEIS3.13 Monoterpenes	FLEXPART Monoterpenes
SOS1999	N/A	N/A
TexAQS2000	N/A	N/A
ICARTT2004	2.26 (0.53)	0.56 (0.55)
TexAQS2006	1.22 (0.41)	0.98 (0.43)

[a]Correlation coefficients R are given in parentheses. Values above 1 imply that the model is larger. The linear fit is an orthogonal distance regression forced through zero. N/A denotes not available.

occurring during the night are accounted for in the used methods. FLEXPART should correctly predict isoprene or monoterpenes observed during the night, if the carryover from daytime emitted isoprene is not longer than 1 h. The carryover is usually small and does not influence the slopes and therefore the nighttime data are included in the analysis presented in Tables 1–3.

[56] The two different methods used to compare the isoprene measurements to the BEIS3.12 emissions database, the mixed boundary layer method (BEIS3.12 in Table 1) and the transport method (FLEXPART in Table 2), yield consistent results within about 30%. The slopes for the FLEXPART method is about 30% higher and the correlation coefficients for both methods are similar. This gives good confidence in the validity of our approaches for this emissions inventory validation. A systematic difference of 30% is clearly within the uncertainties of both methods.

[57] In an average sense, it can be concluded that BEIS3.12 estimates the magnitude of the isoprene emissions very well in Texas in 2006, overestimates in the northeast United States in 2004 and underestimates in the southeast

United States in 1999 and in Texas in 2000. The correlation was the best for the comparison of SOS1999 data in the southeast UNITED STATES and the worst in Texas during TexAQS2000. BEIS3.13 has about 30% lower emissions than BEIS3.12 for all three campaigns, which yields under-predictions for all missions. The correlation between inventory and measurements is slightly improved compared to BEIS3.12.

[58] As was seen earlier and also for the results in Table 1, MEGAN2 is almost a factor of 2 higher than BEIS3.12. For the southeast United States and Texas in 2000 the agreement is very good to within 30%, whereas for the northeast United States and Texas in 2006 MEGAN2 predicts higher emissions than modeled from the measurements. The correlation coefficients are about the same as for the comparison with BEIS3.12 ranging from R = 0.59 to R = 0.68.

[59] The WM2001 inventory under predicts emissions in Texas in the same range as BEIS3.12 with a high correlation coefficient in 2006 and rather low in 2000.

[60] For the monoterpenes (Table 3) the comparison with the two different methods is not as consistent as for isoprene, FLEXPART predicts TexAQS2006 within a few percent as does the mixed boundary layer method, but for ICARTT2004 FLEXPART predicts a factor of 2 lower, whereas the mixed boundary layer method is a factor of 2 higher. This is likely caused by the larger errors involved with the monoterpenes analysis. Overall the comparison for ICARTT2004 and TexAQS2006 is close to a factor of 2, but the correlation coefficients for all comparisons are lower than for isoprene.

7.2. Regional and Interannual Differences

[61] The results in the previous section demonstrated that the isoprene emissions calculated from the inventories generally agree within a factor of 2 with the emissions
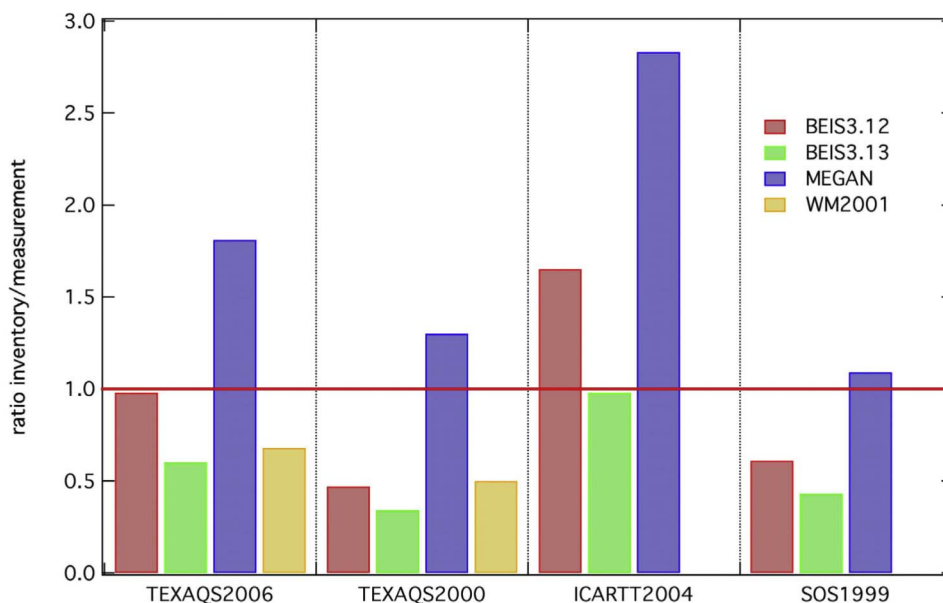
Figure 11. Regression slopes of the isoprene emissions estimated from the inventories versus from the measurements. Values above 1 imply that the inventories are larger. The values of the regression slopes are given in Table 1.
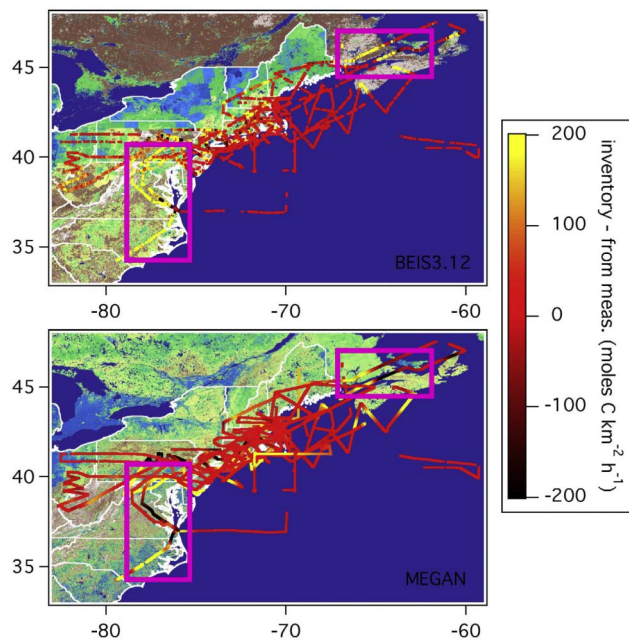
Figure 12. The flight tracks of the NOAA WP-3 during the ICARTT2004 campaign color coded with the difference between the isoprene emissions from (top) BEIS3.12 and (bottom) MEGAN2 and the emissions modeled from the observations. Flight tracks are shown on top of the BEIS3.12 and MEGAN2 base emissions. The pink squares indicate areas where significant differences were observed.

about a factor of 2, but in the same area in 2000 a better agreement with about 30% difference is found as can be seen in Figure 14 showing the TexAQS2000 data.

[64] On average, the inventory/measurement comparison ratio in Texas is about a factor of 2 lower for BEIS3.12 and BEIS3.13 and about 30% lower for MEGAN2 in 2000 compared to 2006 as can be seen in Table 1. This indicates relatively lower emissions modeled from the measurements even after normalizing for temperature and radiation in 2006 than in 2000. A possible reason for the interannual difference in emission strength might be the unusual high temperatures and a resulting drought in 2000. Long drought periods can reduce the local isoprene emissions significantly [*Sharkey et al.*, 1999]. MEGAN2 includes a soil moisture parameterization, which can account for dry periods. No soil moisture data are available and therefore the soil moisture activity factor was set to one in this study for 2000 and 2006, even though 2000 was a hot and dry year. MEGAN2 also includes the past 15 day temperature and radiation, which might be the reason that the relative difference between 2000 and 2006 is smaller than was found for the BEIS3.12 comparison.

[65] Another reason for this interannual difference could be a change in the LAI. For MEGAN2 the standard LAI for the year 2003 was used in all the emission calculations presented so far. LAI data are also available for Texas in 2000 and clear differences between the 2000 and 2003 LAI data were observed. Using the MEGAN2 2000 LAI data to calculate the emissions from MEGAN2 for the Tex-

estimated from the measurements. The data presented here are especially useful for looking at systematic regional differences because of the large number of flights and large area covered. The difference between inventory emissions and the ones modeled from measurements during Tex-AQS2006 and ICARTT2004 are used to color code the flight tracks plotted on the BEIS3.12 base emissions and MEGAN2 emission factors. For SOS1999, no significant local differences were observed and are therefore not shown.
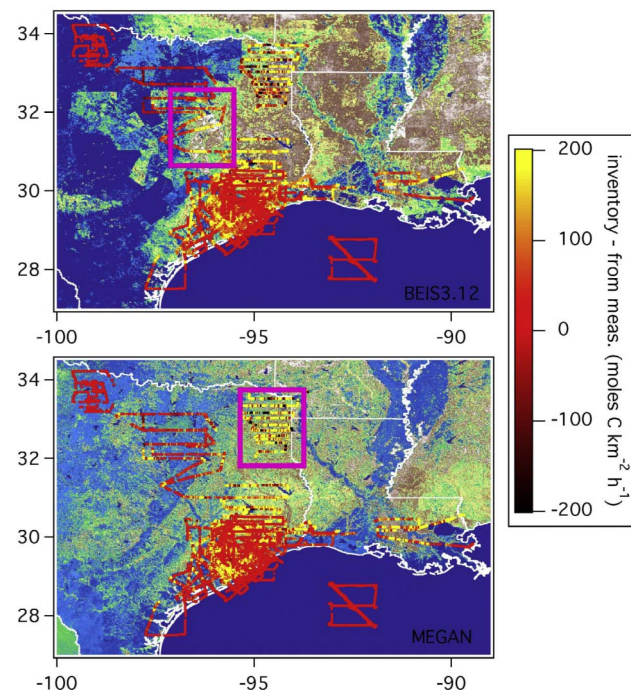
[62] The differences for the northeast United States are shown in Figure 12. Along the U.S.-Canadian border there is a large discontinuity in both the BEIS3.12 and BEIS3.13 base emissions, which is the result of different land-cover data used. This discontinuity at the border is not seen in the MEGAN2 model. Looking at the part of the flight track over Canada, it seems that BEIS3.12 is higher and MEGAN2 somewhat lower than the emissions estimated from the measurements. The same is the case for the flight tracks over the Carolinas, even though MEGAN2 is generally a factor of 2 higher than BEIS3.12.

[63] The Texas results are shown in Figures 13 and 14. For BEIS3.12 and MEGAN2 some areas with significant differences are evident. Especially between Houston and Dallas, an isoprene hot spot is present in BEIS3.12 (and in BEIS3.13 and WM2001), but only small isoprene emissions are found in those areas from the ambient measurements. MEGAN2 on the other hand, does not predict large emissions in this area in better agreement with the observations. In the northeast of Texas in 2006, MEGAN2 clearly is higher than the emissions modeled from the observations by

Figure 13. The flight tracks of the NOAA WP-3 during the TexAQS2006 campaign color coded with the difference between the isoprene emissions from (top) BEIS3.12 and (bottom) MEGAN2 with emissions modeled from the observations. Flight tracks are shown on top of the BEIS3.12 and MEGAN base emissions. The pink squares indicate areas where significant differences were observed.
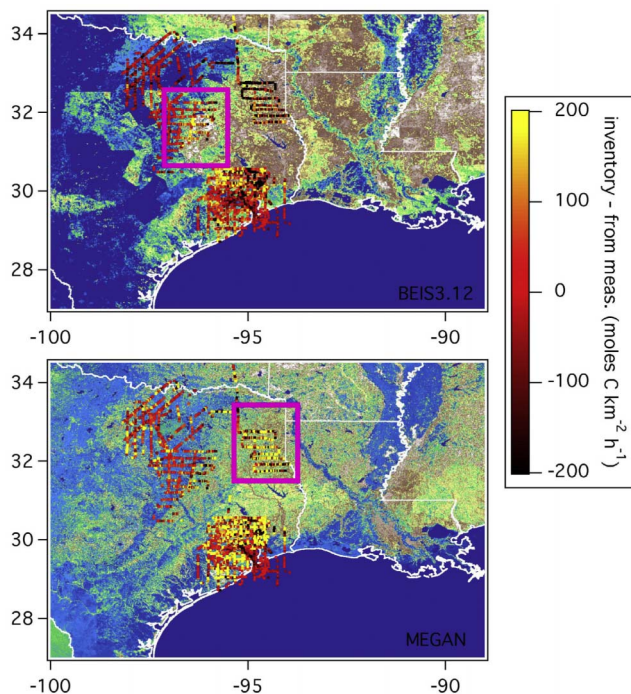
Figure 14. The flight tracks of the NOAA WP-3 during the TexAQS2000 campaign color coded with the difference between the isoprene emissions from (top) BEIS3.12 and (bottom) MEGAN with emissions modeled from the observations. Flight tracks are shown on top of the BEIS3.12 and MEGAN2 base emissions. The pink squares indicate areas where significant differences were observed.

This has two possible explanations: (1) small monoterpene emissions are present in this area that are not included in BEIS3.13 or (2) FLEXPART does not transport the monoterpenes out of the shallow boundary layer to the aircraft altitude.

8. Conclusions and Implications

[68] Airborne isoprene and monoterpene measurements during four different field campaigns in the eastern United States and in Texas were used to evaluate different available emission models (BEIS3.12, BEIS3.12, MEGAN2 and WM2001) using two different approaches. First, a mixed boundary layer method was used: the emissions are modeled from the ambient measurements using the isoprene and monoterpene lifetimes and the boundary layer height. The emission estimates from the measurements are compared to emissions calculated from the models, which are calculated using observations on the aircraft of all the necessary parameters, such as radiation and temperature. Second, a transport model was used: BEIS3.12 was incorporated into the detailed transport model FLEXPART and isoprene mixing ratios are calculated by accumulating all the emissions within the last hour of transport and compared to the measurements. Overall an agreement to better than a factor of 2 was found for all inventories and all campaigns and both methods yielded consistent results.

[69] Generally MEGAN2 is almost a factor of 2 higher than BEIS3.12, which is in turn about 30% higher than BEIS3.13, although there are some regions where MEGAN2 was higher than BEIS3.12. The emissions from

AQS2000 campaign results in about 10% average increase in the isoprene emissions. This changes the slope of the scatterplot of MEGAN2 versus the emissions estimated from the isoprene measurements to 1.40 as compared to 1.30 shown in Table 1 for this comparison. This effect reduces the interannual difference for the MEGAN2 results.

[66] The results for the two campaigns in Texas show that the interannual differences in isoprene emissions can be as large as a factor of 2 and are affecting large areas as well as smaller regions as was observed elsewhere [Levis et al., 2003].
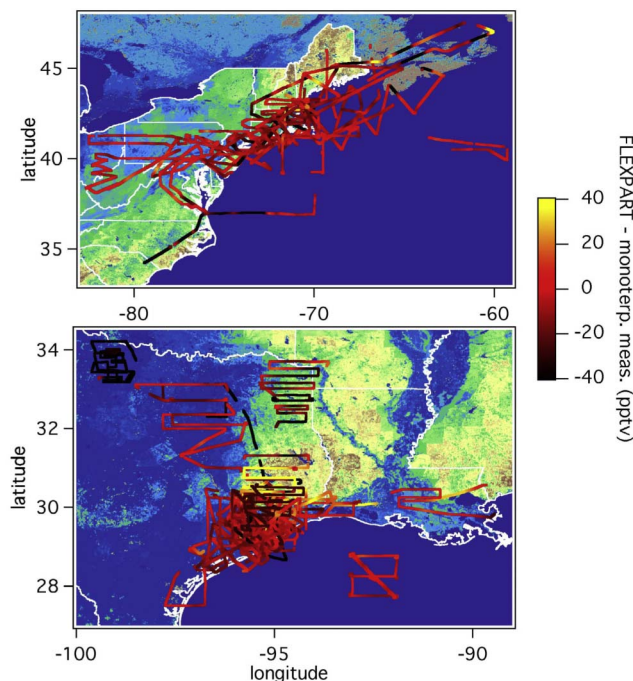
[67] The difference of the monoterpene measurements and FLEXPART calculation is used to color code the flight tracks in Figure 15, which are plotted on top of the BEIS3.13 monoterpene base emissions. As was the case for isoprene, large differences are observed at the border between the United States and Canada and it appears that BEIS3.13 predicts the emissions better on the United States side. In Texas north of Houston, FLEXPART predicts high monoterpene mixing ratios using BEIS3.13, but only small ones were observed. Furthermore, during a flight to the north of Dallas, monoterpene mixing ratios of up to 100 pptv were measured, but FLEXPART predicts less than 10 pptv in this area. This flight was a night flight and therefore long monoterpene lifetimes and a shallow boundary layer could result in elevated mixing ratios. On the other hand, even the FLEXPART tracers that take emissions within 6 h or even 12 h of transport into account are not higher than 15 pptv.

Figure 15. The flight tracks of the NOAA WP-3 during the ICART2004 and TexAQS2006 campaigns color coded with the difference between the monoterpene mixing ratios calculated with FLEXPART and the measured mixing ratios on top of the BEIS3.13 monoterpene base emissions.

MEGAN2 were somewhat higher than the emissions modeled from the isoprene measurements, whereas BEIS3.12 was somewhat lower. This is in contrast to a previous study that found MEGAN to be biased low compared to observations in Harvard forest [*Muller et al.*, 2008]. Other studies find that isoprene emissions over North America inferred from OMI satellite or SCIAMACHY retrievals of formaldehyde [*Millet et al.*, 2008; *Stavrakou et al.*, 2009] are lower than MEGAN.

[70] Using this comparison, some areas were identified, where the differences between the measurements and inventories were larger than average. Examples include the U.S.-Canada border and in Texas to the north of Houston in BEIS3.12 and BEIS3.13, where the inventories are larger than the measurements. In the same areas only small differences were found with MEGAN2, but for example MEGAN2 seems to over predict the emissions in northeast Texas in 2006.

[71] Interannual differences in the emission strength between 2000 and 2006 were observed in Texas, which were likely caused by stronger influence of temperature and drought effects than the models can account for. MEGAN2 takes the previous 15 day temperature and radiation into account, which seems to improve the prediction of the interannual variation. Further improvement was achieved by using the MEGAN2 2000 LAI data for Texas instead of the standard 2003 LAI.

[72] Within the uncertainties of the methods, the biogenic emission inventories that are commonly used for the United States generally agree with the observations within a factor of 2 for isoprene and the monoterpenes. Discrepancies exist for certain areas and interannual changes need to be better accounted for. Due to the large uncertainties, we are unable to recommend one inventory over the other, despite their differences of almost a factor of 2.

[73] Globally, the biosphere is by far the largest source of reactive VOCs and an accurate representation of the emissions in atmospheric chemistry models is therefore critically important. The evaluation of emission inventories is most accurately done using eddy covariance fluxes from surface sites, but this yields information about one location only. Different methods have been used to evaluate emission inventories over larger spatial scales. The comparison between measured and modeled biogenic VOCs can be used to evaluate emission inventories, but requires many different parameters to be modeled correctly including OH concentrations, photoactive radiation, temperatures and boundary level heights. As a result, uncertainties of a factor of 2 in emission inventories can probably not be resolved using this method. The same may be true for evaluations of isoprene emission inventories using formaldehyde retrieved from satellite data, which method is limited by uncertainties in the atmospheric chemistry of formaldehyde and in the satellite retrievals themselves.

[74] Here we used aircraft observations of biogenic VOCs to estimate the emissions in situ and compare them to an emissions inventory model that is constrained by aircraft observations of shortwave radiation and temperature. We also compared observed mixing ratios to those calculated with a Lagrangian transport model. Our methods do still not allow uncertainties of a factor of 2 in emission inventories to be resolved with confidence. Improvements to our method might involve (1) the use of in situ measurements of OH rather than estimates from a parameterization and other measurements, and (2) the use of airborne LIDAR data to estimate boundary layer structure rather than vertical profiles elsewhere during flight. Nevertheless, we expect that such improvements may only provide marginally better results. Better constraints on emission inventories on regional scales may ultimately come from airborne eddy covariance measurements as recently demonstrated by *Karl et al.* [2009], who estimated uncertainties of 40% in the measured fluxes. Such uncertainties are slightly smaller than the uncertainties in the emission inventories themselves and will therefore be needed to provide useful constraints. Regardless, it is expected that significant uncertainties in biogenic emission inventories will remain in the foreseeable future and that, at present, the combination of all available evaluations gives the best assessment of these uncertainties.

[75] On the other hand, given the necessary complexity of the biogenic emission inventories and the evaluation methods an uncertainty of a factor of 2 for isoprene is rather encouraging. Other biogenic VOCs, such as the monoterpenes or oxygenated species like methanol or acetone, are far less certain and a lot more research is needed to assess the emissions of these compounds. Also compared to anthropogenic VOC emission inventories [*Warneke et al.*, 2007], a factor of 2 uncertainty should be considered a good agreement.

Appendix A

[76] The actual emissions in BEIS are calculated according to equation (1) [*Guenther et al.*, 1995]:

$$\text{actual emission} = \text{base emission} \times c_T \times c_L. \quad (A1)$$

[77] The base emissions are shown in Figure 1 and the adjustment factors, c_T and c_L, are calculated as described in the following. The code described here was adapted from a FORTRAN code used in many air quality forecast models such as WRF-Chem. The difference is that measurements made on the aircraft are used as input parameters, which are the solar shortwave radiation, temperature, and solar zenith angle. The calculation of the actual emissions is described in detail to clearly show which assumptions are made and what modeling needs to be done to calculate the emissions from each inventory. The detailed description is also used to point out the differences between the various inventories.
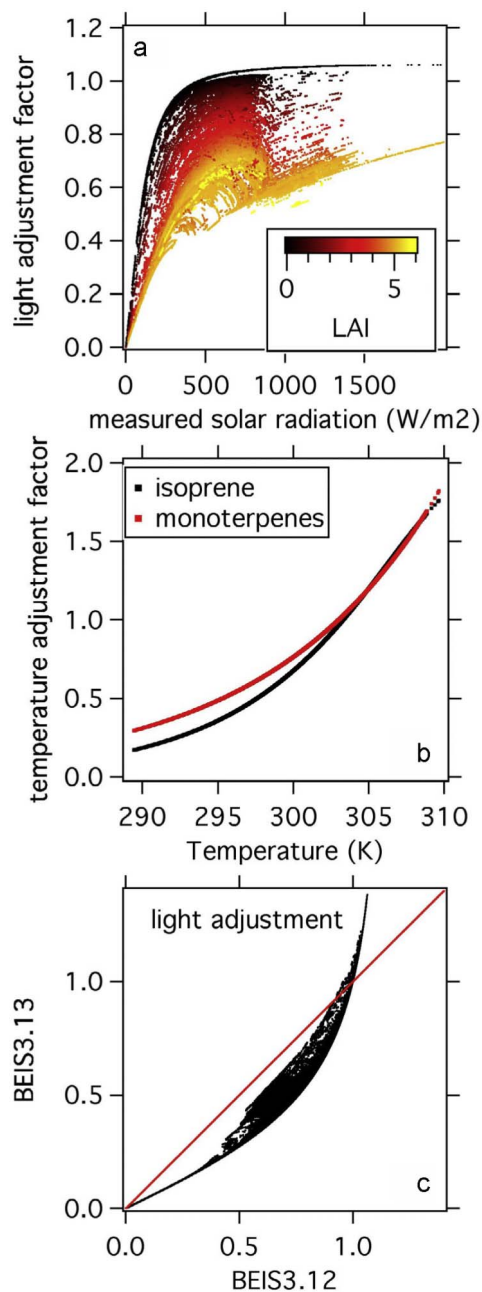
A1. Temperature Adjustment Factor for BEIS 3.12 and BEIS3.13

[78] The temperature adjustment factor for isoprene is

$$c_T = \frac{e^{(37.711 - 0.398570815 \times dT)}}{1 + e^{(91.301 - dT)}} \quad with \quad dT = \frac{28668.514}{T_{ground}}.$$

[79] The temperature adjustment factor for the monoterpenes is

$$c_T = e^{\left(0.09 \times \left(T_{ground} - 303\right)\right)}.$$

Figure A1. (a) The BEIS3.12 light adjustment factor for isoprene for all data from the TexAQS2006 campaign. (b) The temperature adjustment factor for isoprene and the monoterpenes. (c) Comparison of the BEIS3.12 and BEIS3.13 light adjustment factor. The 1:1 line is shown in red.

[80] In this work, the temperature on the ground (T_{ground}) is estimated from the temperature measured onboard the aircraft during take off and landing and missed airport approaches. The results for c_T of the TexAQS2006 campaign are shown in Figure A1b.

A2. Light Adjustment Factor for BEIS3.12 and BEIS3.13

[81] In this section the isoprene light adjustment factor for isoprene is calculated, the monoterpene emissions are not dependent on radiation. The isoprene light adjustment factor for BEIS3 in the WRF-Chem module is calculated with a radiation model that first takes the shortwave solar radiation (t_{solar}: 200–4700 μm) and calculates the photoactive radiation (PAR) in μmol m^{-2} s^{-1} and finds the direct beam (PAR$_{db}$ and PAR$_{dif}$) and diffuse fraction,

$$PAR = PAR_{db} + PAR_{dif},$$

$$PAR_{db} = t_{solar} \times f_{vis} \times f_{vb} \times 4.6,$$

$$PAR_{dif} = t_{solar} \times f_{vis} \times (1 - f_{vb}) \times 4.6,$$

where f_{vis} is the fraction of visible to total radiation, f_{vb} is the fraction of visible light that is direct beam, and the factor 4.6 is to convert from W/m^2 to μmol m^{-2} s^{-1}. To calculate f_{vis} and f_{vb}, the atmospheric pressure (p) in mbar and the solar zenith angle (zen) are used. The following parameters are needed to split t_{solar} into visible and near IR,

$ot = \dfrac{p/1013.25}{\cos(zen)}$	atmospheric optical thickness
$rd_{vis} = 600 \times e^{(-0.185 \times ot)} \times \cos(zen)$	direct beam visible (W/m^2)
$rf_{vis} = 0.42 \times (600 - rd_{vis}) \times \cos(zen)$	diffuse visible (W/m^2)
$wa = 1320 \times 0.077 \times (2 \times ot)^{0.3}$	water absorption in near $-$ IR (W/m^2)
$rd_{ir} = \left(720 \times e^{(-0.06 \times ot)} - wa\right) \times \cos(zen)$	direct beam near $-$ IR $\left(\text{W/m}^2\right)$
$rf_{ir} = 0.65 \times (720 - wa - rd_{ir}) \times \cos(zen)$	diffuse near $-$ IR $\left(\text{W/m}^2\right)$

[82] The total visible and near-IR radiation is calculated using

$r_{vt} = rd_{vis} + rf_{vis}$	total visible radiation
$r_{irt} = rd_{ir} + rf_{ir}$	total near $-$ IR radiation

[83] The fraction of visible to total radiation can then be calculated using

$f_{vis} = \dfrac{r_{vt}}{(r_{vt} + r_{irt})}$	fraction of visible to total radiation
$ratio = \dfrac{t_{solar}}{(r_{vt} + r_{irt})}$	ratio of "actual" to clear sky solar radiation

[84] Now the fraction of the visible radiation that is direct beam can be calculated,

$f_{vb} = \dfrac{rd_{vis}}{r_{vt}} \times 0.941124$	for ratio ≥ 0.89
$f_{vb} = \dfrac{rd_{vis}}{r_{vt}} \times 9.55 \times 10^{-3}$	for ratio ≤ 0.21
$f_{vb} = \dfrac{rd_{vis}}{r_{vt}} \times \left(1 - \left(\dfrac{0.9 - ratio}{0.7}\right)^{2/3}\right)$	for $0.21 \geq ratio \geq 0.89$

[85] The calculated PAR$_{db}$, PAR$_{dif}$ and their sum along the flight track are plotted versus the measured shortwave solar radiation in Figure A2 for the TexAQS2006 data. It can be seen that at low shortwave solar radiation, which occurs at large solar zenith angles and cloudy conditions, PAR becomes mainly diffuse.

[86] Using PAR, split into direct beam and diffuse fractions as shown in Figure A2, together with the LAI, which can be extracted from data in BEIS3 along the flight track,
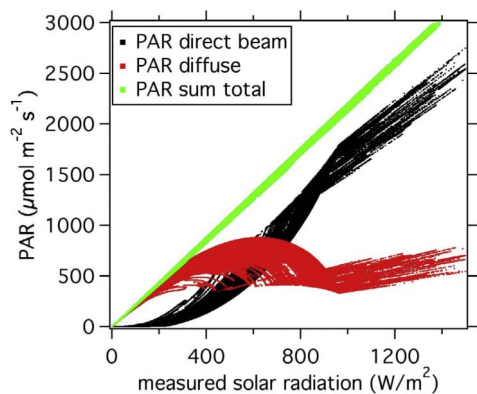
Figure A2. The direct beam and diffuse PAR calculated for the solar radiation measured during TexAQS2006.

the PAR that falls on leaves in the sun and leaves in the shade can be estimated.

$$k_{be} = 0.5 \times \sqrt{1 + \tan(zen)^2}$$
$$\alpha = 0.8$$
$$k_d = 0.68$$
$$canPAR_{scat} = 0.5 \times PAR_{db} \times e^{\left(-\alpha^2 \times k_{be} \times LAI\right)} - e^{\left(-k_{be} \times LAI\right)}$$
$$canPAR_{dif} = \frac{0.5 \times PAR_{dif} \times \left(1 - e^{\left(-\alpha^2 \times k_{be} \times LAI\right)}\right)}{\left(\alpha^2 \times k_{be} \times LAI\right)}$$
$$PAR_{shade} = canPAR_{scat} + canPAR_{dif}$$
$$PAR_{sun} = k_{be} \times PAR_{db} + PAR_{shade}$$
$$PAR_{sun} = k_{be} \times (PAR_{db} + PAR_{dif}) + PAR_{shade}$$

PAR_{sun} in BEIS3.12 includes PAR_{dif}, which is actually a mistake that was corrected in BEIS3.13.

[87] Using LAI the fraction of leaves in the sun or shade can be estimated:

$$frac_{sun} = \frac{\left(1 - e^{\left(-k_{be} \times LAI\right)}\right)/k_{be}}{LAI} \quad \text{fraction of leaves that are sunlit}$$

$$frac_{shade} = 1 - frac_{sun} \quad \text{fraction of leaves that are shaded}$$

[88] The isoprene emission light adjustment factor for the fraction of leaves in the sun and the fraction in the shade can now be calculated using the formulation from *Guenther et al.* [1995],

$$c_L = frac_{sun} \times c_{guen}(PAR_{sun}) + frac_{shade} \times c_{guen}(PAR_{shade})$$
light adjustment factor.

[89] In the determination of c_{guen} lies the major difference between BEIS3.12 and BEIS3.13. The newer version uses the updated reference of *Guenther et al.* [1999] instead of the older *Guenther et al.* [1993] reference,

$$c_{guen}(PAR) = \frac{0.0028782 * PAR}{\sqrt{1 + 0.00000729 * PAR^2}} \quad \text{used in BEIS3.12}$$

$$c_{guen}(PAR) = \frac{0.001 * 1.42 * PAR}{\sqrt{1 + 0.001^2 * PAR^2}} \quad \text{used in BEIS3.13}$$

[90] For PAR < 0.01 and zenith angles > 89 degrees, c_L is set to zero and for very small LAI < 0.1 c_L is set to

$c_{guen}(PAR_{db} + PAR_{dif})$. In Figure A1 the resulting c_T and c_L for the TexAQS2006 campaign are plotted versus the ground temperature and the shortwave solar radiation, respectively. Shown are 1 s aircraft data for the whole campaign, resulting in a large number of data points. In Figure A1a the light adjustment factor is color coded by LAI and it can be seen that at high LAI, when it is assumed that leaves in the lower part of the canopy are shaded, c_L is reduced relative to low LAI values. Figure A1c shows the scatterplot of the light adjustment factor from BEIS3.12 versus BEIS3.13. In Figure A1b the isoprene and monoterpene temperature adjustment factors are shown.

Appendix B

[91] The actual emissions in MEGAN2 are calculated according to equation (B1)

$$\text{Emission} = [\varepsilon][\gamma][\rho], \tag{B1}$$

	extinction coefficient for direct beam
	leaf absorptivity
	extinction coefficient for diffuse
	scattered PAR in the canopy (μmol m^{-2} s^{-1})
	diffuse PAR in the canopy (μmol m^{-2} s^{-1})
	PAR on shaded leaves (μmol m^{-2} s^{-1})
	PAR on sunlit leaves in BEIS3.13 (μmol m^{-2} s^{-1})
	PAR on sunlit leaves in BEIS3.12 (μmol m^{-2} s^{-1})

[92] The emission factor ε is taken from the data as shown in Figure 1, the canopy loss and production term ρ is set to 0.96 and the emission activity factor γ is calculated as described in the following. A more detailed description of MEGAN and this calculation are given by *Guenther et al.* [2006].

[93] The emission activity factor γ is calculated from

$$\gamma = \gamma_{CE} \times \gamma_{age} \times \gamma_{SM} = \gamma_P \times \gamma_T \times \gamma_{LAI} \times \gamma_{age} \times \gamma_{SM},$$

where γ_{CE} is the canopy environment emission activity factor, γ_{age} is the leaf age and γ_{SM} the soil moisture emission activity factor. γ_{CE} is calculated from the temperature γ_T, the PPFD (photosynthetic photon flux density) γ_P and the LAI γ_{LAI} emission activity factors. The following calculation was adapted from a FORTRAN code used in MEGANv2.03.

B1. Leaf Area Index Emission Activity Factor

[94] The γ_{LAI} can be calculated by:

$$\gamma_{LAI} = \frac{0.49 \times LAI}{\sqrt{\left(1 + 0.2 \times LAI^2\right)}},$$

where leaf area index (LAI) in m^2 m^{-2} is taken from the current months LAI data used in MEGAN2 from 2003. The
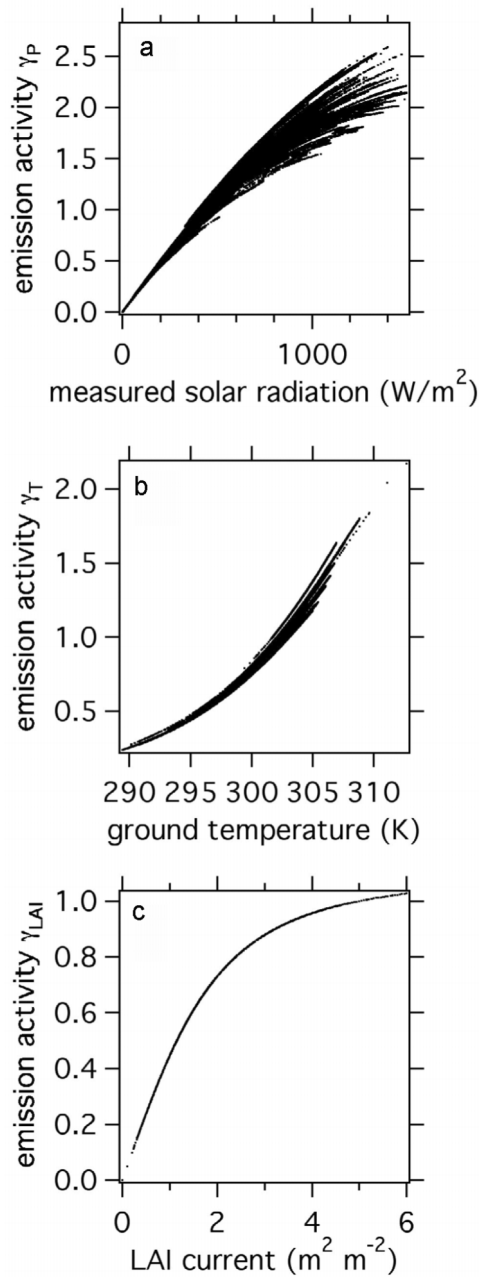
Figure B1. The MEGAN (a) light, (b) temperature, and (c) LAI emission activity factors for all data from the TexAQS2006 campaign.

γ_{LAI} for all data from the TexAQS2006 campaign is shown in Figure B1.

B2. Photosynthetic Photon Flux Density Emission Activity Factor

[95] The γ_P can be calculated by:

$$\gamma_P = \sin(sel) \times \left[2.46 \times \left(1 + 0.0005 \times \left(P_{daily} - 400\right)\right) \times \phi - 0.9 \times \phi^2\right]$$

$$\phi = \frac{P_{ac}}{\sin(sel) \times P_{toa}}$$

$$P_{ac} = t_{solar} \times 4.766 \times 0.5$$

$$P_{toa} = 3000 + 99 \times \cos\left[2 \times 3.14 \times \frac{(DOY - 10)}{365}\right]$$

where PFPD is photosynthetic photon flux density. The solar elevation angle (sel), the shortwave radiation (t_{solar}), the day of the year (DOY) and an average past shortwave radiation (P_{daily}) is required. Here, P_{daily} is calculated as a past 15 day average from the ECMWF data input to the FLEXPART model, which was manipulated to output P_{daily} for each grid box for each hour during the entire TexAQS2006 and ICARTT2004 campaigns. For SOS1999 P_{daily} was estimated using temperature measurements from the ground site close to Nashville and for TexAQS2000 using data from the LaPorte site. The γ_P for all data from TexAQS2006 is shown in Figure C.

B3. Temperature Emission Activity Factor

[96] The γ_T can be calculated by:

$$\gamma_T = \frac{E_{opt} \times c_{T2} \times e^{(c_{T1} \times x)}}{\left[c_{T2} - c_{T1} \times \left(1 - e^{(c_{T2} \times x)}\right)\right]}$$

$$x = \left[\left(\frac{1}{T_{opt}}\right) - \left(\frac{1}{T_{ground}}\right)\right]/0.00831$$

$$E_{opt} = 1.75 \times e^{\left(0.08 \times \left(T_{daily} - 297\right)\right)}$$

$$T_{opt} = 313 + 0.6 \times \left(T_{daily} - 297\right)$$

[97] The ground temperature (T_{ground}) in K and an average past temperature (T_{daily}) in K are required, where the past 15 day average temperature was calculated in the same way as the past solar radiation using FLEXPART and the ground sites. C_{T1} is 80 and C_{T2} is 200. The result of the γ_T calculation for all data from TexAQS2006 is also shown in Figure B1.

B4. Leaf Age and Soil Moisture Emission Activity Factor

[98] The leaf age γ_{age} and the soil moisture γ_{SM} emission activity factors were set to:

$$\gamma_{age} = \gamma_{SM} = 1.$$

above canopy PPFD transmission (μmol m^{-2} s^{-1})

above canopy PPFD (μmol m^{-2} s^{-1})

PPFD at the top of the atmosphere (μmol m^{-2} s^{-1})

References

Atkinson, R., et al. (2005), Summary of evaluated kinetic and photochemical data for atmospheric chemistry, report, Subcomm. on Gas Kinetic Data Eval. for Atmos. Chem., Int. Union of Pure and Appl. Phys., London. (Available at http://www.iupac-kinetic.ch.cam.ac.uk/)

Atkinson, R., et al. (2006), Evaluated kinetic and photochemical data for atmospheric chemistry: Volume II—Gas phase reactions of organic species, *Atmos. Chem. Phys.*, 6, 3625–4055.

Brock, C. A., et al. (2002), Particle growth in the plumes of coal-fired power plants, *J. Geophys. Res.*, 107(D12), 4155, doi:10.1029/2001JD001062.

Brock, C. A., et al. (2008), Sources of particulate matter in the northeastern United States in summer: 2. Evolution of chemical and microphysical properties, *J. Geophys. Res.*, 113, D08302, doi:10.1029/2007JD009241.

Brown, S. S., et al. (2005), Aircraft observations of daytime NO$_3$ and N$_2$O$_5$ and their implications for tropospheric chemistry, *J. Photochem. Photobiol., A*, 176(1–3), 270–278.

Chen, G., et al. (2005), An investigation of the chemistry of ship emission plumes during ITCT 2002, *J. Geophys. Res.*, 110, D10S90, doi:10.1029/2004JD005236.

de Gouw, J., and C. Warneke (2007), Measurements of volatile organic compounds in the Earth's atmosphere using proton-transfer-reaction mass spectrometry, *Mass Spectrom. Rev.*, 26(2), 223–257, doi:10.1002/mas.20119.

de Gouw, J. A., P. D. Goldan, C. Warneke, W. C. Kuster, J. M. Roberts, M. Marchewka, S. B. Bertman, A. A. P. Pszenny, and W. C. Keene (2003), Validation of proton transfer reaction-mass spectrometry (PTR-MS) measurements of gas-phase organic compounds in the atmosphere during the New England Air Quality Study (NEAQS) in 2002, *J. Geophys. Res.*, 108(D21), 4682, doi:10.1029/2003JD003863.

de Gouw, J. A., et al. (2005), Budget of organic carbon in a polluted atmosphere: Results from the New England Air Quality Study in 2002, *J. Geophys. Res.*, 110, D16305, doi:10.1029/2004JD005623.

de Gouw, J. A., et al. (2006), Volatile organic compounds composition of merged and aged forest fire plumes from Alaska and western Canada, *J. Geophys. Res.*, 111, D10303, doi:10.1029/2005JD006175.

Edwards, G. D., et al. (2003), Chemical ionization mass spectrometer instrument for the measurement of tropospheric HO$_2$ and RO$_2$, *Anal. Chem.*, 75(20), 5317–5327, doi:10.1021/ac034402b.

Ehhalt, D. H., and F. Rohrer (2000), Dependence of the OH concentration on solar UV, *J. Geophys. Res.*, 105(D3), 3565–3571, doi:10.1029/1999JD901070.

Fehsenfeld, F. C., et al. (2006), International Consortium for Atmospheric Research on Transport and Transformation (ICARTT): North America to Europe—Overview of the 2004 summer field study, *J. Geophys. Res.*, 111, D23S01, doi:10.1029/2006JD007829.

Geron, C., et al. (2000), A review and synthesis of monoterpene speciation from forests in the United States, *Atmos. Environ.*, 34, 1761–1781, doi:10.1016/S1352-2310(99)00364-7.

Goldan, P. D., D. D. Parrish, W. C. Kuster, M. Trainer, S. A. McKeen, J. Holloway, B. T. Jobson, D. T. Sueper, and F. C. Fehsenfeld (2000), Airborne measurements of isoprene, CO, and anthropogenic hydrocarbons and their implications, *J. Geophys. Res.*, 105(D7), 9091–9105, doi:10.1029/1999JD900429.

Guenther, A. B., and A. J. Hills (1998), Eddy covariance measurement of isoprene fluxes, *J. Geophys. Res.*, 103(D11), 13,145–13,152, doi:10.1029/97JD03283.

Guenther, A., P. R. Zimmerman, P. C. Harley, R. K. Monson, and R. Fall (1993), Isoprene and monoterpene emission rate variability: Model evaluation and sensitivity analysis, *J. Geophys. Res.*, 98(D7), 12,609–612,617, doi:10.1029/93JD00527.

Guenther, A., et al. (1995), A global model of natural volatile organic compound emissions, *J. Geophys. Res.*, 100(D5), 8873–8892, doi:10.1029/94JD02950.

Guenther, A., B. Baugh, G. Brasseur, J. Greenberg, P. Harley, L. Klinger, D. Serça, and L. Vierling (1999), Isoprene emission estimates and uncertainties for the Central African EXPRESSO study domain, *J. Geophys. Res.*, 104(D23), 30,625–30,639, doi:10.1029/1999JD900391.

Guenther, A., et al. (2006), Estimates of global terrestrial isoprene emissions using MEGAN (Model of Emissions of Gases and Aerosols from Nature), *Atmos. Chem. Phys.*, 6, 3181–3210.

Hawes, A. K., et al. (2003), Airborne observations of vegetation and implications for biogenic emission characterization, *J. Environ. Monit.*, 5(6), 977–983, doi:10.1039/b308911h.

Henze, D. K., and J. H. Seinfeld (2006), Global secondary organic aerosol from isoprene oxidation, *Geophys. Res. Lett.*, 33, L09812, doi:10.1029/2006GL025976.

Jacob, D. J. (2000), Heterogeneous chemistry and tropospheric ozone, *Atmos. Environ.*, 34, 2131–2159, doi:10.1016/S1352-2310(99)00462-8.

Jacob, D. J., B. D. Field, E. M. Jin, I. Bey, Q. Li, J. A. Logan, R. M. Yantosca, and H. B. Singh (2002), Atmospheric budget of acetone, *J. Geophys. Res.*, 107(D10), 4100, doi:10.1029/2001JD000694.

Jacob, D. J., et al. (2005), Global budget of methanol: Constraints from atmospheric observations, *J. Geophys. Res.*, 110, D08303, doi:10.1029/2004JD005172.

Karl, T. G., A. Guenther, R. J. Yokelson, J. Greenberg, M. Potosnak, D. R. Blake, and P. Artaxo (2007), The tropical forest and fire emissions experiment: Emission, chemistry, and transport of biogenic volatile organic compounds in the lower atmosphere over Amazonia, *J. Geophys. Res.*, 112, D18302, doi:10.1029/2007JD008539.

Karl, T., et al. (2009), Emissions of volatile organic compounds inferred from airborne flux measurements over a megacity, *Atmos. Chem. Phys.*, 9, 271–285.

Lelieveld, J., et al. (2008), Atmospheric oxidation capacity sustained by a tropical forest, *Nature*, 452(7188), 737–740, doi:10.1038/nature06870.

Levis, S., C. Wiedinmyer, G. B. Bonan, and A. Guenther (2003), Simulating biogenic volatile organic compound emissions in the Community Climate System Model, *J. Geophys. Res.*, 108(D21), 4659, doi:10.1029/2002JD003203.

McKeen, S., et al. (2005), Assessment of an ensemble of seven real-time ozone forecasts over eastern North America during the summer of 2004, *J. Geophys. Res.*, 110, D21307, doi:10.1029/2005JD005858.

Millet, D. B., D. J. Jacob, K. F. Boersma, T.-M. Fu, T. P. Kurosu, K. Chance, C. L. Heald, and A. Guenther (2008), Spatial distribution of isoprene emissions from North America derived from formaldehyde column measurements by the OMI satellite sensor, *J. Geophys. Res.*, 113, D02307, doi:10.1029/2007JD008950.

Muller, J. F., et al. (2008), Global isoprene emissions estimated using MEGAN, ECMWF analyses and a detailed canopy environment model, *Atmos. Chem. Phys.*, 8, 1329–1341.

Palmer, P. I., et al. (2006), Quantifying the seasonal and interannual variability of North American isoprene emissions using satellite observations of the formaldehyde column, *J. Geophys. Res.*, 111, D12315, doi:10.1029/2005JD006689.

Parrish, D. D., et al. (2009), Overview of the Second Texas Air Quality Study (TexAQS II) and the Gulf of Mexico Atmospheric Composition and Climate Study (GoMACCS), *J. Geophys. Res.*, 114, D00F13, doi:10.1029/2009JD011842.

Pfister, G. G., L. K. Emmons, P. G. Hess, J. F. Lamarque, J. J. Orlando, S. Walters, A. Guenther, P. I. Palmer, and P. J. Lawrence (2008), Contribution of isoprene to chemical budgets: A model tracer study with the NCAR CTM MOZART-4, *J. Geophys. Res.*, 113, D05308, doi:10.1029/2007JD008948.

Pierce, T. E., and P. S. Waldruff (1991), Pc-Beis—A personal-computer version of the biogenic emissions inventory system, *J. Air Waste Manage. Assoc.*, 41(7), 937–941.

Pierce, T., C. Geron, L. Bender, R. Dennis, G. Tonnesen, and A. Guenther (1998), Influence of increased isoprene emissions on regional ozone modeling, *J. Geophys. Res.*, 103(D19), 25,611–25,629, doi:10.1029/98JD01804.

Rohrer, F., and H. Berresheim (2006), Strong correlation between levels of tropospheric hydroxyl radicals and solar ultraviolet radiation, *Nature*, 442(7099), 184–187, doi:10.1038/nature04924.

Ryerson, T. B., et al. (1998), Emissions lifetimes and ozone formation in power plant plumes, *J. Geophys. Res.*, 103(D17), 22,569–522,583, doi:10.1029/98JD01620.

Ryerson, T. B., E. Williams, and F. Fehsenfeld (2000), An efficient photolysis system for fast-response NO$_2$ measurements, *J. Geophys. Res.*, 103(D21), 26,447–426,461, doi:10.1029/2000JD000389.

Ryerson, T. B., et al. (2003), Effect of petrochemical industrial emissions of reactive alkenes and NO$_x$ on tropospheric ozone formation in Houston, Texas, *J. Geophys. Res.*, 108(D8), 4249, doi:10.1029/2002JD003070.

Sharkey, T. D., et al. (1999), Weather effects on isoprene emission capacity and applications in emissions algorithms, *Ecol. Appl.*, 9(4), 1132–1137, doi:10.1890/1051-0761(1999)009[1132:WEOIEC]2.0.CO;2.

Song, J., et al. (2008), Comparisons of modeled and observed isoprene concentrations in southeast Texas, *Atmos. Environ.*, 42, 1922–1940, doi:10.1016/j.atmosenv.2007.11.016.

Stark, H., B. M. Lerner, R. Schmitt, R. Jakoubek, E. J. Williams, T. B. Ryerson, D. T. Sueper, D. D. Parrish, and F. C. Fehsenfeld (2007), Atmospheric in situ measurement of nitrate radical (NO$_3$) and other photolysis rates using spectroradiometry and filter radiometry, *J. Geophys. Res.*, 112, D10S04, doi:10.1029/2006JD007578.

Stavrakou, T., et al. (2009), Global emissions of non-methane hydrocarbons deduced from SCIAMACHY formaldehyde columns through 2003–2006, *Atmos. Chem. Phys.*, 9(11), 3663–3679.

Stohl, A., and D. J. Thomson (1999), A density correction for Lagrangian particle dispersion models, *Boundary Layer Meteorol.*, 90(1), 155–167, doi:10.1023/A:1001741110696.

Stohl, A., et al. (2005), Technical note: The Lagrangian particle dispersion model FLEXPART version 6.2, *Atmos. Chem. Phys.*, 5, 2461–2474.

Tanner, D. J., A. Jefferson, and F. L. Eisele (1997), Selected ion chemical ionization mass spectrometric measurement of OH, *J. Geophys. Res.*, *102*(D5), 6415–6425, doi:10.1029/96JD03919.

Warneke, C., et al. (2003), Validation of atmospheric VOC measurements by proton-transfer-reaction mass spectrometry using a gas-chromatographic preseparation method, *Environ. Sci. Technol.*, *37*(11), 2494–2501, doi:10.1021/es026266i.

Warneke, C., et al. (2004), Comparison of daytime and nighttime oxidation of biogenic and anthropogenic VOCs along the New England coast in summer during New England Air Quality Study 2002, *J. Geophys. Res.*, *109*, D10309, doi:10.1029/2003JD004424.

Warneke, C., et al. (2007), Determination of urban volatile organic compound emission ratios and comparison with an emissions database, *J. Geophys. Res.*, *112*, D10S47, doi:10.1029/2006JD007930.

Wiedinmyer, C., et al. (2001), A land use database and examples of biogenic isoprene emission estimates for the state of Texas, USA, *Atmos. Environ.*, *35*, 6465–6477, doi:10.1016/S1352-2310(01)00429-0.

————————————

E. Atlas, Marine and Atmospheric Chemistry Division, Rosenstiel School of Marine and Atmospheric Sciences, University of Miami, 4600 Rickenbacker Causeway, Miami, FL 33149, USA.

J. Brioude, J. A. de Gouw, F. C. Fehsenfeld, P. D. Goldan, J. S. Holloway, W. C. Kuster, S. McKeen, J. Peischl, T. B. Ryerson, H. Stark, M. Trainer, and C. Warneke, Chemical Sciences Division, ESRL, NOAA, 325 Broadway, R/CSD7, Boulder, CO 80305, USA. (carsten.warneke@noaa.gov)

L. Del Negro, Department of Chemistry, Lake Forest College, 555 N. Sheridan Rd., Lake Forest, IL 60045-2338, USA.

A. B. Guenther and C. Wiedinmyer, ACD, NCAR, Boulder, CO 80301, USA.

A. T. C. Hanks, Department of Geosciences, University of Louisiana at Monroe, Monroe, LA 71209, USA.

A. Hansel and A. Wisthaler, Institut für Ionenphysik und Angewandte Physik, Universität Innsbruck, Technikerstrasse 25, A-6020 Innsbruck, Austria.

L. G. Huey, School of Earth and Atmospheric Sciences, Georgia Institute of Technology, Atlanta, GA 30332-0340, USA.